D2. GEOLOGY OF NORTH RAY CRATER

By George E. Ulrich

CONTENTS

ILLUSTRATIONS

TABLES

INTRODUCTION

North Ray crater was the primary sampling target of the last of three traverses made during the Apollo 16 mission. Its apparent youth minimizes the chance of contamination by ejecta from younger craters; its deep exposures, 230 m into the subsurface, reveal stratigraphic differences to approximately that depth. Orbital and surface photographs illustrating the vertical sequence of units exposed in the wall of North Ray crater, together with the rocks and soils collected on its rim and ejecta blanket and the crew's first-hand observations, provide the controlling data for interpreting a stratigraphic model in this area of the landing site. This model is extended to the larger region explored by Apollo 16 in Ulrich and Reed (this volume).

PHYSIOGRAPHIC SETTING

North Ray crater lies at the foot of Smoky mountain and is one of the highest sampling sites in the landing area. Its setting is well illustrated from a surface perspective on plate 11 (pan 34). Station 4, on Stone mountain, is at approximately the same elevation; the rim of South Ray crater, 10 km to the south, is about 170 m lower (fig. 1). About 1 km across, North Ray crater straddles a ridge approximately 50 m high and a little narrower than the crater rim. The crest of this ridge, informally named North Ray ridge, is nearly parallel to the base of Smoky mountain. Its similarity in morphology to Smoky mountain and to the Descartes highlands in general was not recognized until after the mission when orbital photography with low-sun-angle illumination became available (fig. 2). The top of the ridge is 400 m below the top of Smoky mountain, which suggests that the ridge may be a downfaulted segment of the mountain and therefore that North Ray crater may expose material from part of the Descartes mountains in its walls.

That part of the crater interior visible from the rim is shown by the postmission topographic map (fig. 3). The crest is rounded but falls off rapidly to the steep crater wall, whose upper slopes are generally convex, ranging from 27" at the top to 34" in the lower half. Precipitous drops in the foreground slopes below the rim crest made photographing the lowest parts of the crater wall impossible. Only the upper 60 percent of the crater wall is observable from the vantage point at station 11 (figs. 3, 4). The rounded form of the crater rim, the smooth walls with few blocky areas, and the predominance of breccias in the observable rocks on the surface are evidence that the target materials impacted by North Ray crater were breccias of relatively low strength.

BLOCK DISTRIBUTION AND ROCK TYPES

The concentration of blocks on the rim of North Ray crater was considerably lower than anticipated. The low frequency of fragments was observed on the approach to the crater rim. Fragments range from 25 m to less than 1 m in maximum diameter. Most of the large boulders observable on postmission orbital photographs, mapped here on figure 5, had been identified on premission photographs. Within 10 m of the site of panorama 18 (pl. 8), fragments 10 cm and larger cover 4.3 percent of the surface (figs. 4, 6A); at station 13, 0.75 km away, they cover only 0.5 percent with about one-fourth as many fragments (fig. 6B and panorama 23, pl. 7). Nearly 70 percent of the fragments counted at these stations are rounded (fig. 6; table 1). At station 11, more than 20 percent are larger than 20 cm in diameter, at station 13, only 10 percent.

All the blocks with discernible textures are clastic in appearance. Their matrices range from dark to light gray, as seen in the black-and-white photographs. The

TABLE 1.—*Distribution of blocks at North Ray crater by size and shape*

[Number of blocks counted and percentage of total within 10 m of center of station panoramas. Data from figure 6]

Shape	10–20 cm	20–50 cm	>50 cm	Total	Shape percent
Station 11—rim crest					
Rounded	145	35	0	180	69.0
Subangular	44	11	0	55	21.0
Angular	13	3	10	26	10.0
Total	202	49	10	261	
Size percent	77.4	18.8	3.8		100.0
Station 13—outer ejecta blanket					
Rounded	41	6	0	47	68.1
Subangular	13	1	0	14	20.3
Angular	8	0	0	8	11.6
Total	62	7	0	69	
Size percent	89.9	10.1	0		100.0

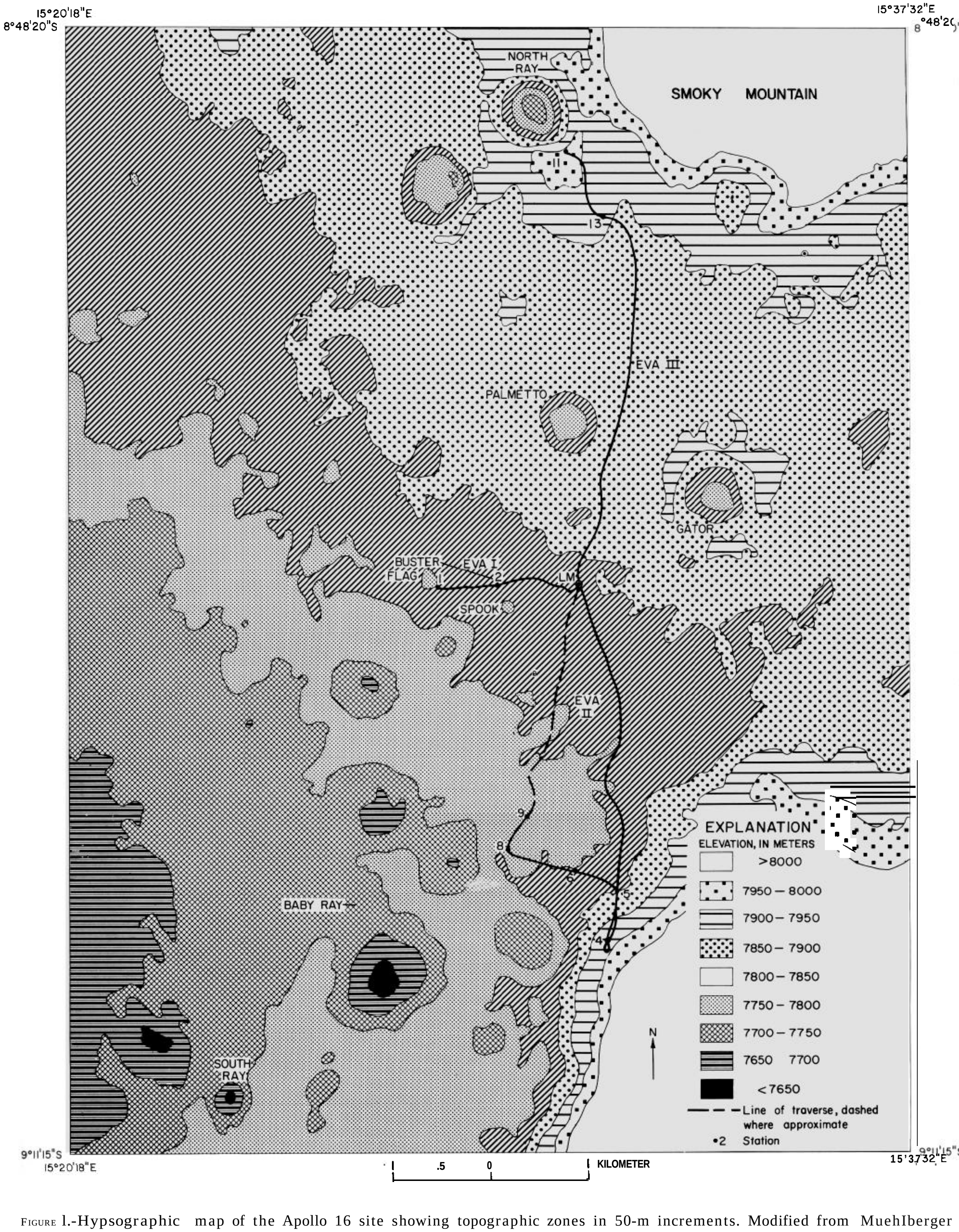

FIGURE 1.-Hypsographic map of the Apollo 16 site showing topographic zones in 50-m increments. Modified from MuehIberger and others (1972) and AFGIT (1973). Copyright 1973 by the American Association for the Advancement of Science.

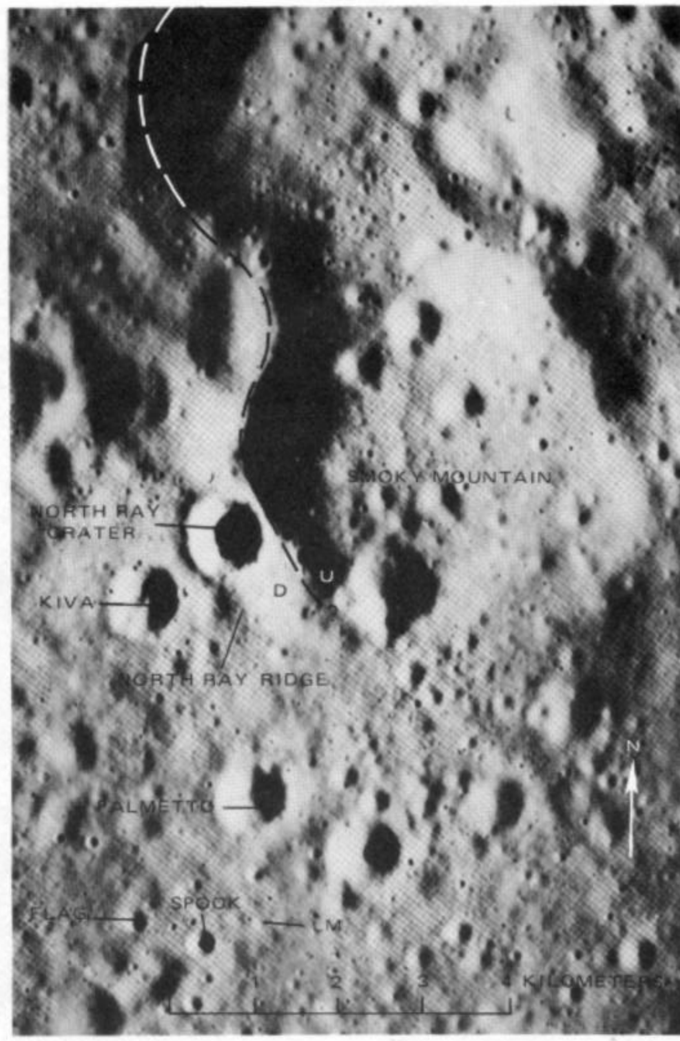

FIGURE 8.--Northern part of Apollo 16 landing site, showing principal named features. Dashed line, possible fault; U. upthrown side; D, downthrown side. Apollo 16 panoramic camera frame 4558, sun elevation 16”. From Ulrich (1973) Reprinted with permission of Pergamon

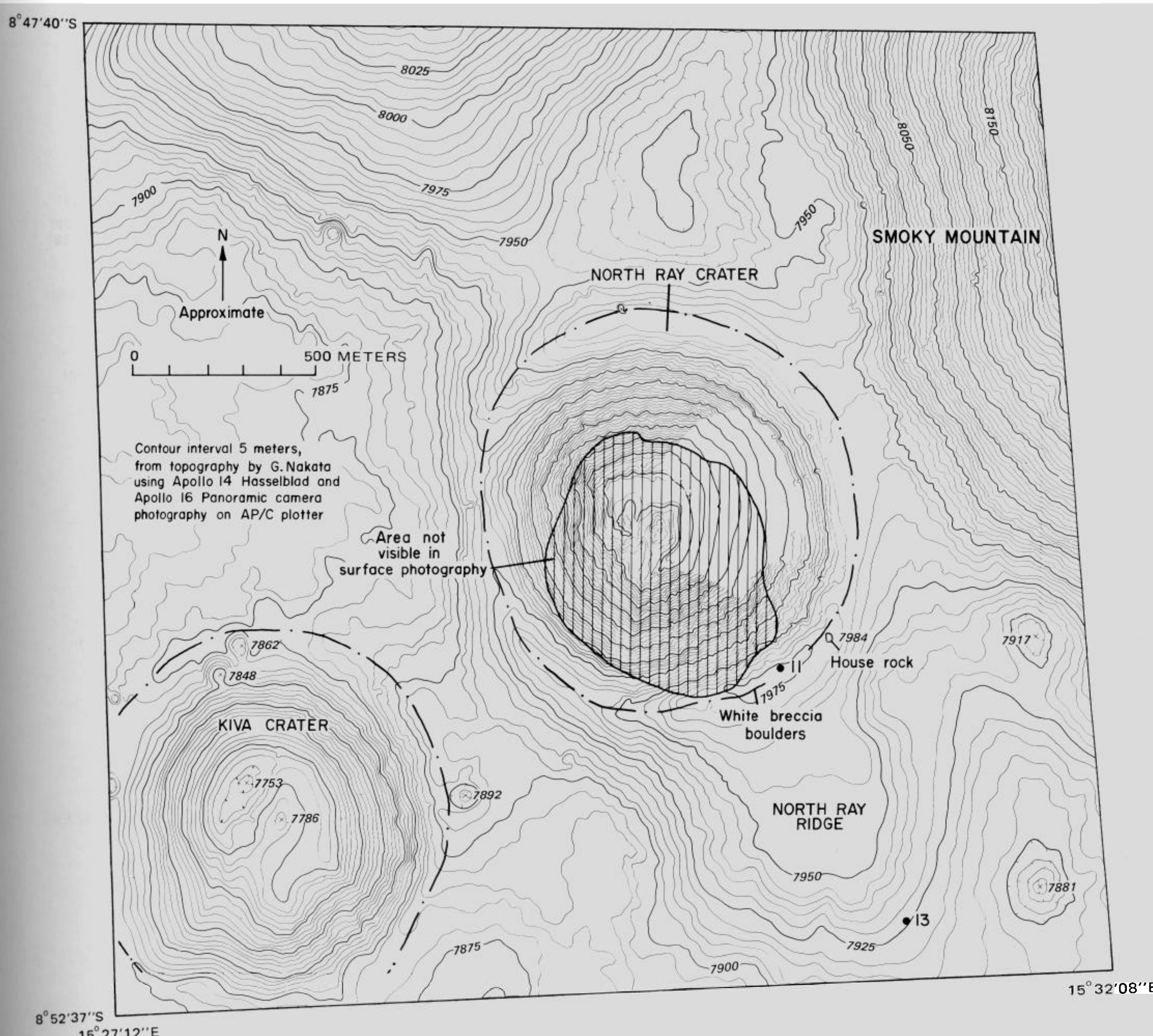

FIGURE 3.-Topographic map of North Ray crater showing station localities and area visible from rim. Contour interval 5 m. Topography by G. M. Nakata from Apollo 16 panoramic camera frames 4618 and 4623. From Ulrich (1973). Reprinted with permission of Pergamon Press.

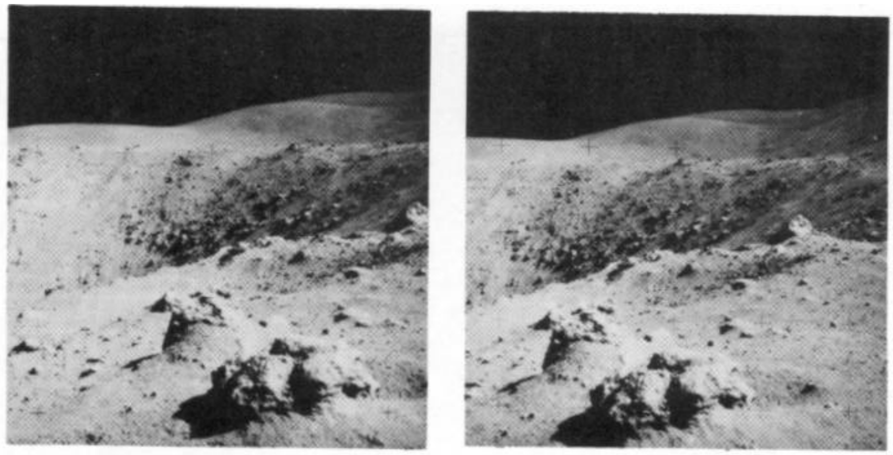

Figure: 4.-Stereopair showing northeast wall of North Ray crater from east panorama station. Foreground shows typical slopes inside rim crest. AS16-106-17301, 17302.

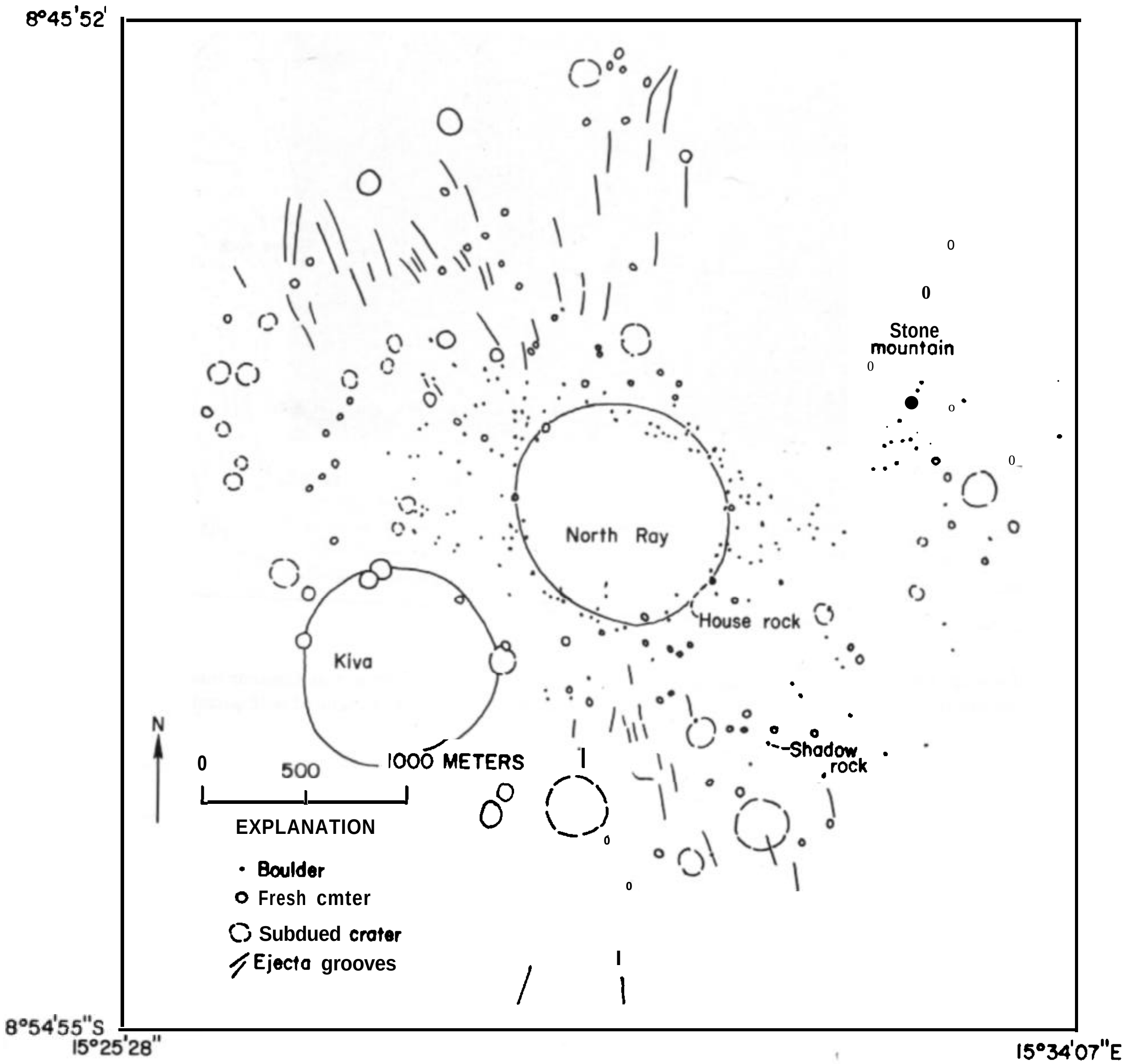

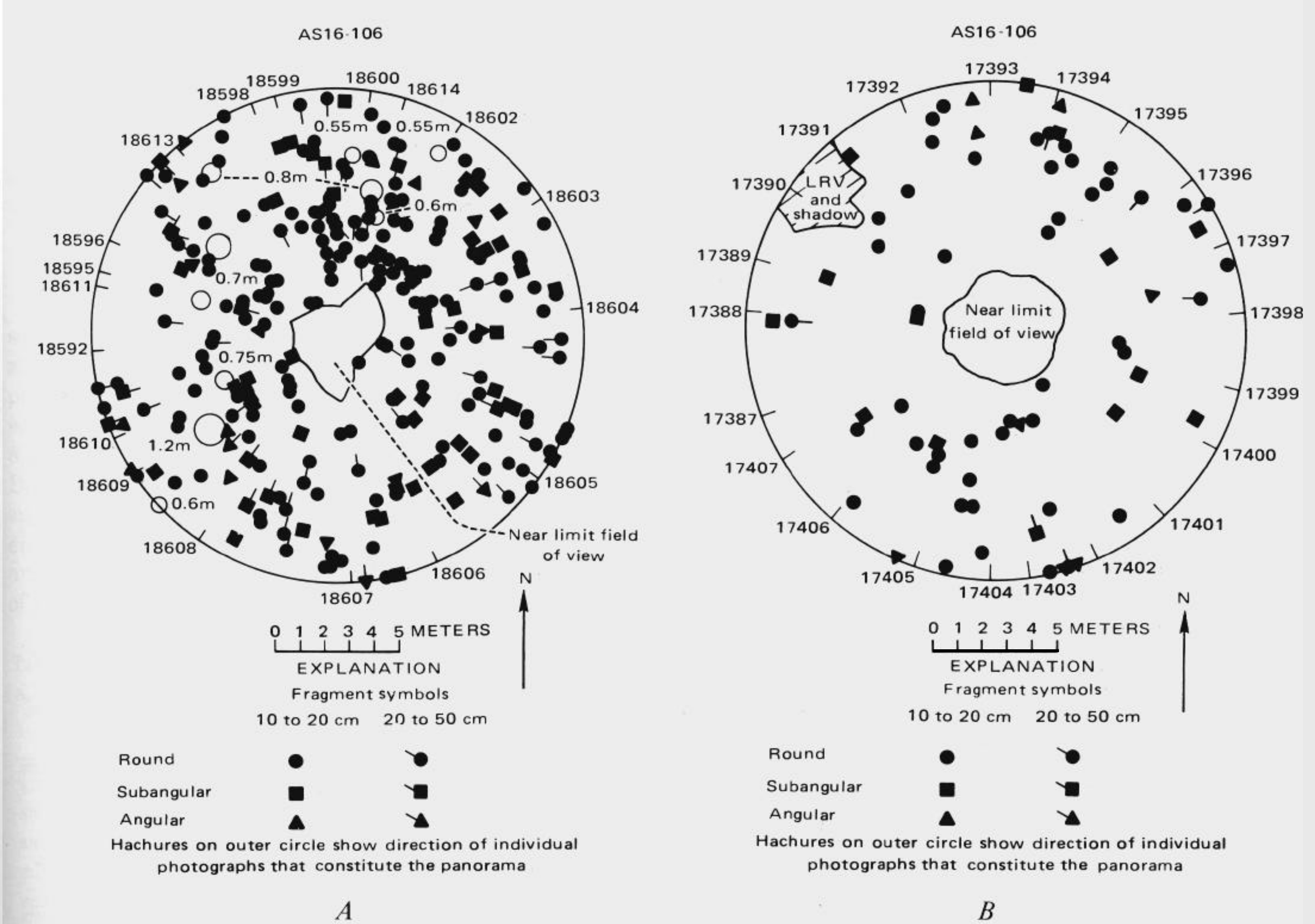

FIGURE 6.-Block distribution within 10 m of sites of station 11 and station 13 panoramas. ***A,*** Station 11. B, Station 13. From Muehlberger and others, 1972.

(FIGURE **5.—Map** of boulders, craters, and ejecta grooves in North Ray crater area. Data from Apollo 16 panoramic camera frames 4563 and 4623.

dark-matrix rocks consistently exhibit angular edges and pronounced jointing, and few have soil fillets developed at their bases (figs. 7-9).

Light-matrix boulders are distinctly more rounded more crudely jointed, and more deeply filleted by soil inferred to be their own residual debris (figs. 10 and 11). The rock sample characteristics, discussed below and by Wilshire and others (this volume), reflect similar differences in coherence or friability. Megascopically and microscopically, textures indicate that variations in rock colors and coherence are produced by differences in amounts of impact melt incorporated in the rocks and in rates of cooling.

Of more than 800 rocks in the near field of four photographic panoramas taken on the rim and ejecta blanket of North Ray crater, 70 to 90 percent are relatively light colored (fig. 12). These include the light- and medium-gray-matrix breccias (B1, B2, and B, of Wilshire and others, this volume) and probably some igneous and metaclastic rocks (C, and C2,) that are indistinguishable from the light-matrix breccias in surface photographs. Rocks consisting largely of glass (class G of Wilshire and others, this volume) may be counted as dark rocks (dark-matrix breccias, B, and B,) except where large amounts of light-colored soil adhered to their surfaces. The percentage of dark rocks increases from about 10 in the western part of the southeast rim (panorama 19 and sketch, pl. 8) to nearly 30 at a location midway between the White breccia boulders and House rock. About 20 percent of the fragments at Shadow rock are dark.

SAMPLE LOCALITIES

In order to reconstruct the stratigraphic sequence in North Ray crater, the distribution and concentration of the several rock types with respect to their location on the crater wall and floor were studied. The sampled area is subdivided into four localities, the White cia boulders, the Interboulder area, the House rock area and the Shadow rock area (fig. 13), whose names were derived from descriptive terms used by the crew. All but Shadow rock are on the crater rim crest. Shadow rock is approximately 0.75 km southeast of the

TABLE 2.—*Rock samples greater than 2 g from the House rock area*

Sample No.	Weight group (g) 2–25	25–100	100+	Classification (Wilshire and others, this volume, table 1)	Geologic significance
67915	----	----	×	B_4	Representative of House and Outhouse rocks.
67935	----	----	×	[1](C_2)	Metaclastic matrix from Outhouse rock.
67936	----	×	----	C_1	Same as 67935, in impact-spall zone.
67937	----	×	----	B_4	Dark-matrix breccia from impact spall zone.
67945	×	----	----	B_4	Rock from "east-west split."
67946	×	----	----	(B_4)	Do.
67947	×	----	----	(B_4)	Do.
67955	----	----	×	B_1	Light-matrix clast from Outhouse rock.
67956	×	----	----	C_1	Igneous fragment from Outhouse rock.
67975	----	----	×	B_2	Fragment in soil near Outhouse rock.

( ) Provisional classification by Wilshire and others, this volume, table 1.

TABLE 3.—*Rock samples greater than 2 g from the White breccia boulders area*

Sample No.	Weight group (g) 2–25	25–100	100+	Classification (Wilshire and others, this volume, table 1)	Geologic significance
67016	----	----	×	[1]$B_3(B_2)$	Large loose rock on crater rim crest.
67025	×	----	----	$B_2(B_3)$	Coherent fragment, possibly from 67016.
67035	----	----	×	B_2	"Three-rock" breccia 20 m inside rim crest.
67215	----	----	×	Unclass	Unopened rock in padded bag.
67415	----	----	×	B_1	Friable rock at base of light-matrix breccia boulder.
67435	----	----	×	[2](B_4)	Glass-coated; may be dark- and light-matrix breccia.
67455	----	----	×	B_2	Fragments off top of 6 m light-matrix breccia boulder.
67475	----	----	×	B_4	Clast from the same boulder as 67455.
67485	×	----	----	(C_2)	Fragment in soil near 67455 light-matrix boulder.
67486	×	----	----	(B_1)	Do.
67487	×	----	----	(C_2)	Do.
67488	×	----	----	(C_2)	Do.
67489	×	----	----	(C_2)	Do.
67515	----	×	----	B_2	Breccia in rake sample near 67455 light-matrix boulder.
67516	×	----	----	$B_2(B_1)$	Do.
67517	×	----	----	$B_2(B_1)$	Do.
67518	×	----	----	$B_2(B_1)$	Do.
67519	×	----	----	$B_2(B_1)$	Do.
67525	×	----	----	$B_2(B_1)$	Do.
67526	×	----	----	$B_2(B_1)$	Do.
67527	×	----	----	$B_2(B_1)$	Do.
67539	×	----	----	$B_2(B_1)$	Do.
67549	----	×	----	B_2	Do.
67555	×	----	----	B_2	Do.
67556	----	×	----	B_2	Do.
67557	×	----	----	Unclass	Do.
67558	×	----	----	Unclass	Do.
67559	----	×	----	(C_2)	Olivine basalt* in rake sample near 67455 boulder.[3]
67565	×	----	----	C_2	Basalt* in rake sample near 67455 boulder.
67566	×	----	----	C_2	Do.
67567	×	----	----	G	Breccia in rake sample near 67455 boulder.
67568	×	----	----	G	Do.
67569	×	----	----	G	Do.
67575	×	----	----	G	Do.
67576	×	----	----	G	Do.
67605	----	×	----	B_2	Fragment from soil sample in rake area.
67615	×	----	----	C_2	Basalt* in rake sample 10 m inside rim crest.
67616	×	----	----	C_2	Do.
67617	×	----	----	C_2	Basaltic breccia* in rake sample 10 m inside rim crest.
67618	×	----	----	C_2	Do.
67619	×	----	----	C_2	Do.
67625	×	----	----	C_2	Metaclastic rock in rake sample 10 m inside rim crest.
67626	×	----	----	G	Breccia in rake sample 10 m inside rim crest.
67627	----	×	----	G	Do.
67628	----	×	----	G	Do.
67629	----	×	----	G	Basalt* clast from light-matrix breccia.
67635	×	----	----	B_1	Breccia in rake sample 10 m inside rim crest.
67636	×	----	----	B_1	Do.
67637	×	----	----	B_1	Do.
67638	×	----	----	B_2	Do.
67639	×	----	----	B_2	Do.
67646	×	----	----	B_2	Do.
67647	----	×	----	Unclass	Do.
67648	×	----	----	B_2	Do.
67655	×	----	----	B_2	Do.
67665	×	----	----	(B_3)	Do.
67666	×	----	----	B_2	Do.
67667	×	----	----	C_2	Ultramafic?* in rake sample 10 m inside rim crest
67668	×	----	----	C_2	Basaltic breccia* in rake sample 10 m inside rim crest
67669	×	----	----	(B_3)	Breccia in rake sample 10 m inside rim crest
67676	×	----	----	C_2	Basalt* in rake sample 10 m inside rim crest

$B_2(B_3)$ Alternative classification by Wilshire and others (this volume).
( ) Provisional classification by Wilshire and others (this volume).
Interpretation from Smith and Steele (1972).

crest, but still on continuous North Ray ejecta. For each of the four areas, the rock samples weighing more than 2 g are tabulated and their geologic significance indicated in tables 2 to 5. Their occurrence by rock type is graphically compared in figure 14. The larger soil samples and their location and geologic significance are given in table 6.

HOUSE ROCK AREA

The largest boulder visited and one established as a sampling target before the mission is House rock. It is an angular, predominantly dark-matrix boulder, approximately 25 m long and 12 m high, at the northeastern limit of the crater-rim-crest traverse area (figs. 8, 13; pl. 8, pan 28). It was so named when Astronaut Duke, on first observing it at station 11, compared its size to that of a house. Less than 1 m away on the south end of House rock is a 3-m boulder of similar texture, anonymously named Outhouse rock, the source of most of the rock samples collected at this locality.

TABLE 4.—*Rock samples greater than 2 g from the Interboulder area*

Sample No.	2–25g	25–100	100+	Classification (Wilshire and others, this volume)	Geologic significance
67015	----	----	×	[1]$B_3(B_2)$	Large loose rock inside rim crest.
67055	----	----	×	$B_2(B_3)$	Collected for abundant black clasts (more than 67035).
67075	----	----	×	B_1	Found as two broken pieces of white shocked rock.
67095	----	----	×	G	Collected for appearance as "really black glass."
67115	----	----	×	[2](B_3)	Same location as 67095; more rounded.
67235	----	----	×	Unclass	Unopened rock in padded bag.
67705	×	----	----	(G)	Fragment in rake soil on rim crest.
67706	×	----	----	Unclass	Do.
67715	×	----	----	B_4	Basalt* probably clast from light-matrix breccia.[3]
67716	×	----	----	B_4	Breccia, probable clast from light-matrix breccia.
67717	×	----	----	B_4	Do.
67718	----	×	----	(B_3)	Do.
67719	×	----	----	B_4	Do.
67725	×	----	----	B_4	Breccia in rake sample on rim crest.
67726	×	----	----	B_4	Do.
67728	×	----	----	G	Fragment in rake sample on rim crest.
67729	----	×	----	G	Do.
67735	×	----	----	$B_3(B_3)$	Do.
67736	×	----	----	C_2	Olivine basalt with ultramafic inclusion; zapped on all sides.*
67737	×	----	----	B_4	Basalt* probable clast from light-matrix breccia.
67738	×	----	----	B_4	Do.
67739	×	----	----	B_4	Fragment in rake sample on rim crest.
67745	×	----	----	B_4	Basalt* in rake sample on rim crest.
67746	×	----	----	C_2	Norite?* in rake sample on rim crest.
67747	×	----	----	C_2	Troctolite?* in rake sample on rim crest.
67748	×	----	----	C_2	Fragment in rake sample on rim crest.
67749	×	----	----	B_2	Breccia in rake sample on rim crest.
67755	×	----	----	B_2	Do.
67756	×	----	----	B_2	Do.
67757	×	----	----	B_2	Do.
67758	×	----	----	B_2	Do.
37759	×	----	----	B_2	Do.
67766	×	----	----	B_2	Do.
67769	×	----	----	B_2	Do.
67775	×	----	----	B_2	Do.
67776	×	----	----	B_2	Do.

[1]$B_3(B_2)$ Alternative classification by Wilshire and others (this volume).
[2]( ) Provisional classification by Wilshire and others (this volume).
[3]Interpretation from Smith and Steele (1972)

TABLE 5.—*Rock samples greater than 2 g from the Shadow rock area, station 13, on outer North Ray ejecta*

Sample No.	2–25g	25–100	100+	Classification (Wilshire and others, this volume)	Geologic significance
60017	----	----	×	[1]$B_4(B_3)$	Large rock broken off from 2 m area on southwest side of Shadow rock.
63335	----	×	----	[2](B_3)	Chip rock broken off from 2 m area on southwest side of Shadow rock.
63355	----	×	----	B_4	Do.
63505	×	----	----	(B_4)	Fragment in rake soil 5–10 m west of Shadow rock
63506	×	----	----	C_1	Do.
63507	×	----	----	B_3	Do.
63508	×	----	----	B_3	Do.
63509	×	----	----	B_2	Do.
63525	×	----	----	(B_4)	Do.
63526	×	----	----	(B_4)	Do.
63527	×	----	----	(B_4)	Do.
63528	×	----	----	(B_4)	Do.
63529	×	----	----	(B_4)	Do.
63535	×	----	----	(B_4)	Do.
63537	×	----	----	(C_2)	Do.
63538	----	×	----	(C_2)	Do.
63545	×	----	----	(C_2)	Do.
63546	×	----	----	(B_4)	Do.
63547	×	----	----	(C_2)	Do.
63549	----	×	----	(C_2)	Do.
63555	×	----	----	(B_4)	Do.
63556	×	----	----	(C_2)	Do.
63557	×	----	----	(B_4)	Do.
63558	×	----	----	(C_2)	Do.
63559	×	----	----	(G)	Do.
63566	×	----	----	(G)	Do.
63567	×	----	----	(G)	Do.
63568	×	----	----	(G)	Do.
63575	×	----	----	(G)	Do.
63577	×	----	----	$(B_4(C_2))$	Do.
63578	×	----	----	(B_3)	Do.
63579	×	----	----	(B_3)	Do.
63585	----	×	----	(C_2)	Do.
63587	×	----	----	(B_3)	Do.
63588	×	----	----	(B_2)	Do.
63589	×	----	----	$(B_3(B_2))$	Do.
63595	×	----	----	(B_3)	Do.
63596	×	----	----	(B_3)	Do.
63597	×	----	----	(B_3)	Do.
63598	×	----	----	(B_3)	Do.

[1]$B_4(B_3)$ Alternative classification by Wilshire and others (this volume)
[2]( ) Provisional classification by Wilshire and others (this volume).

TABLE 6.—*North Ray crater soil samples greater than 26 g*

Sample No.*	White breccia boulder area	Interboulder area	House rock area	Shadow rock area	Geologic significance
63320–4	----	----	----	×	"Shadowed" soil on surface under northwest overhang of Shadow rock.
63340–4	----	----	----	×	Soil beneath 63320 under northwest overhang of Shadow rock.
63500–4	----	----	----	×	Rake soil 5–10 m west of Shadow rock.
67010	----	×	----	----	Residue in sample collection bag No. 7
67020	×	----	----	----	Residue in Buddy Secondary Life Support System bag with rock 67016.
67030–4	×	----	----	----	Residue in sample bag with rock 67035.
67410	×	----	----	----	Residue in sample bag with rock 67415.
67450	×	----	----	----	Residue in sample bag with rock 67455.
67460–4	×	----	----	----	Fillet at boulder from which 67455 and 67475 were collected.
67480–4	×	----	----	----	Reference soil for comparison with 67460; same location as sample 67510.
67510–4	×	----	----	----	Soil in rake sample near large, light-matrix breccia boulder.
67600–4	×	----	----	----	Rake soil collected about 25 m east of 67510; inside rim crest.
67610	×	----	----	----	Soil in rake sample from same location as 67600.
67700–4	----	×	----	----	Rake soil from half way between White breccia boulders and House rock.
67710–4	----	×	----	----	Soil in rake sample from same location as 67700.
67910	----	----	×	----	Residue in sample collection bag No. 4.
67940–4	----	----	×	----	Soil from "east-west split" between House and Outhouse rocks.

*-4 indicates sample was sieved in LRL into newly numbered fractions, 1 through 4, for less than 1 mm, 1–2 mm, 2–4 mm, and 4–10 mm, respectively.

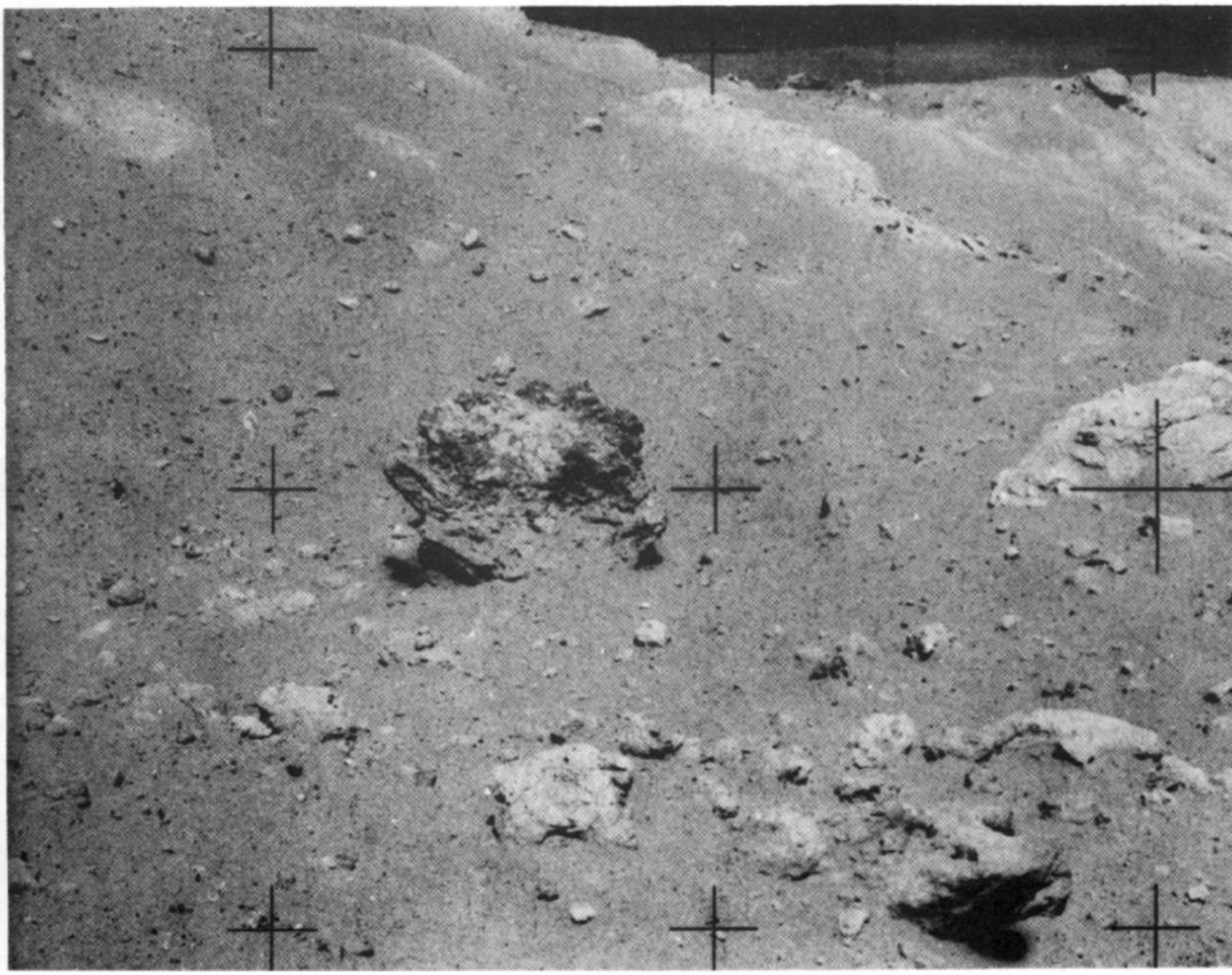

FIGURE 7.-Dark-matrix breccia boulder in White breccia boulder area. For location see panorama 19, pl. 8.

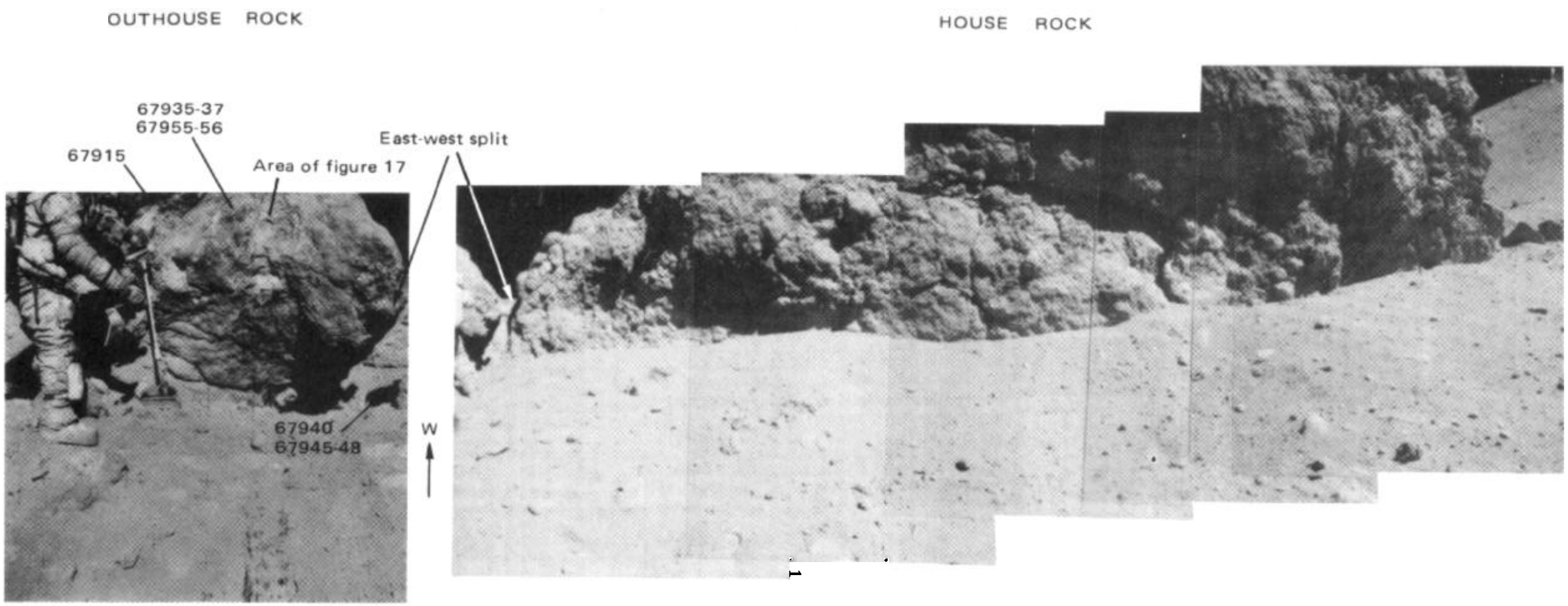

FIGURE 8.—House rock and Outhouse rock panorama at station 11, showing east face of dark-matrix breccia boulders. Note lack of fillet at base and angular, jointed faces. AS16–116–18653 (left) and 106–17349 to 19354.

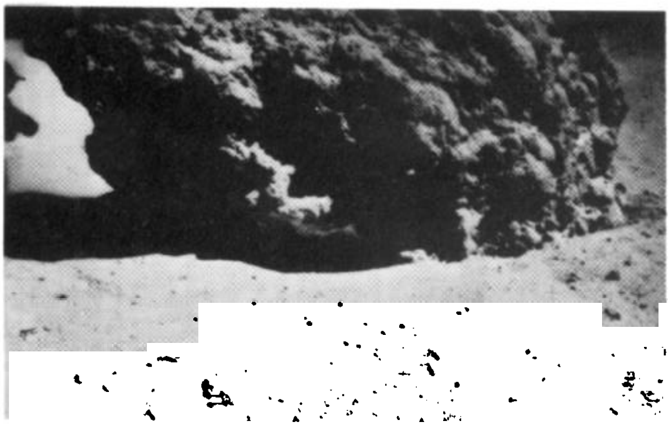

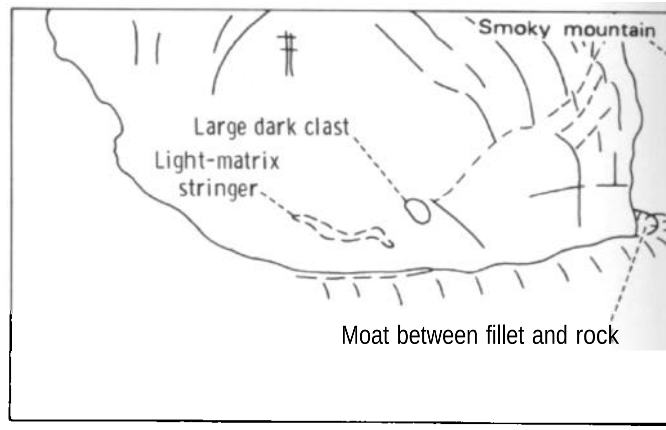

A B

FIGURE %--Shadow rock panorama at station 13. *A,* South face of 5-m-wide boulder of dark-matrix breccia. AS16- 106-17413 to 17415. B. Sketch map of fractures and clasts.

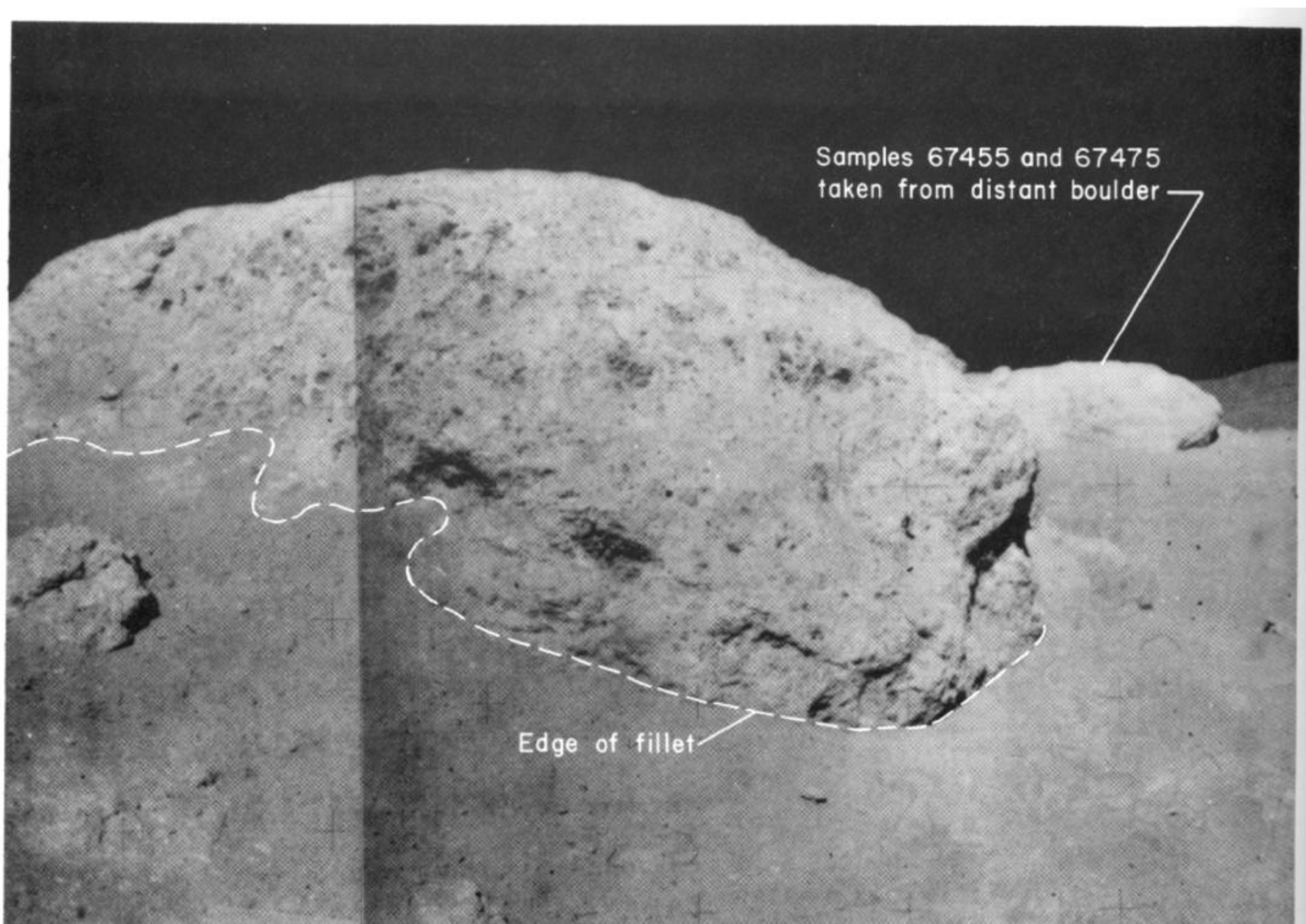

FIGURE 10.--white breccia boulders showing rounded outlines and deeply filleted margins. AS16-106- 17325 and 17326.

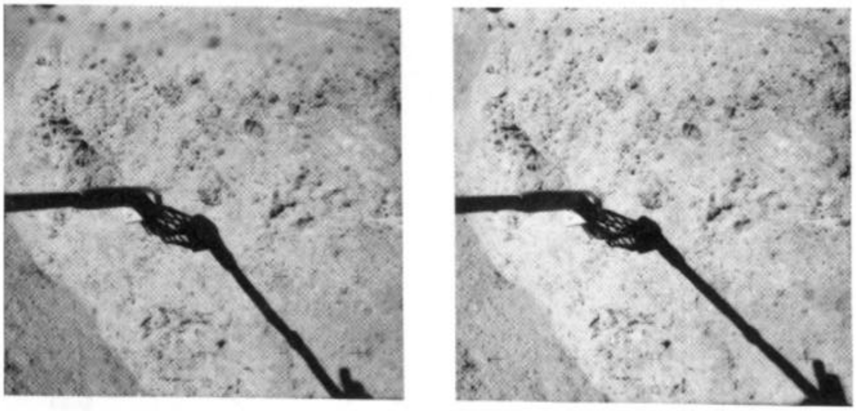

A

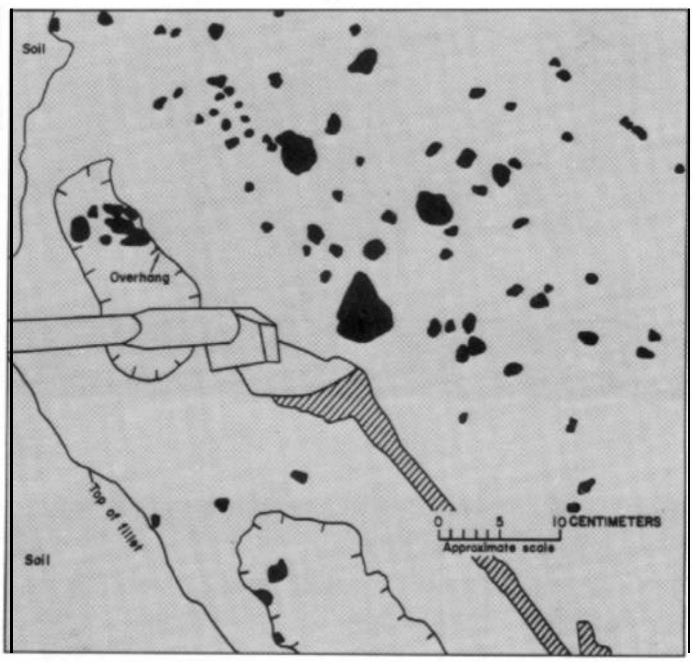

B

FIGURE 11.-Surface texture and distribution of dark clasts, White breccia boulder. ***A,*** Stereopair showing surface texture. AS16 106-17327 to 17328. B, Sketch map showing distinction of dark clasts and top of fillet.

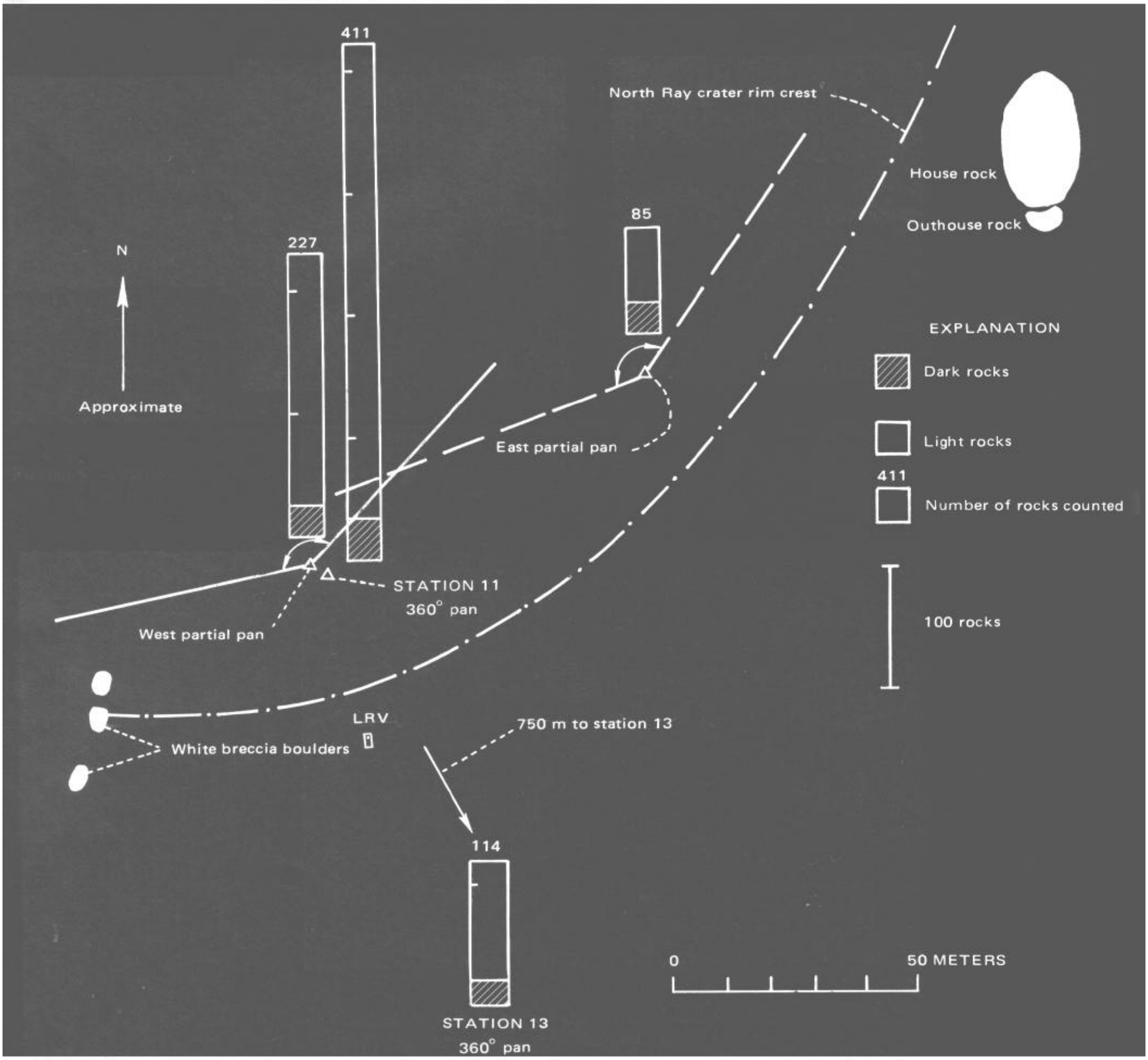

FIGURE 12.-Proportions of light and dark fragments counted in surface panoramas. Data from plate 7, pan 23, plate 8, pans 18 and 19, and plate 9, pan 20. Boulder map from Sutton (this volume).

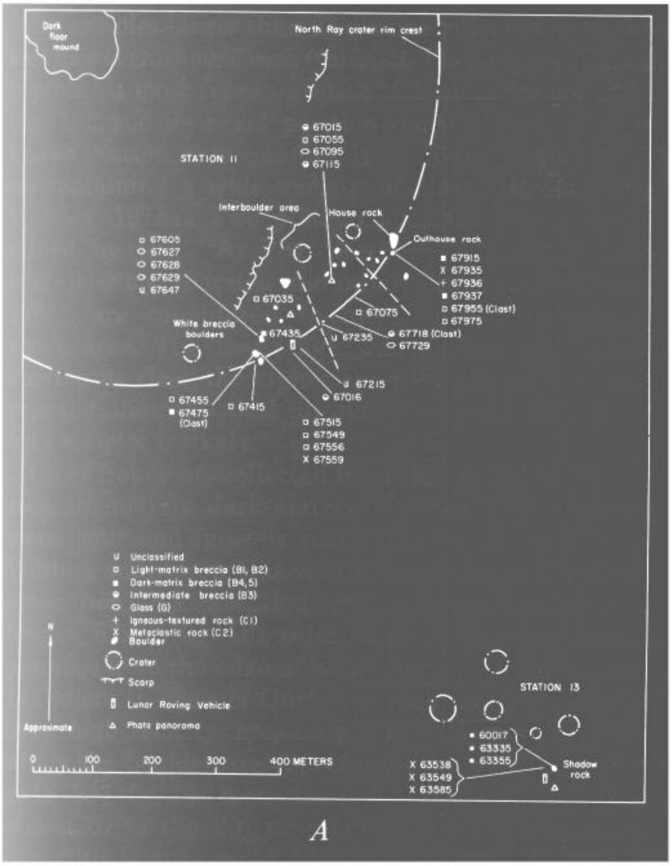

A

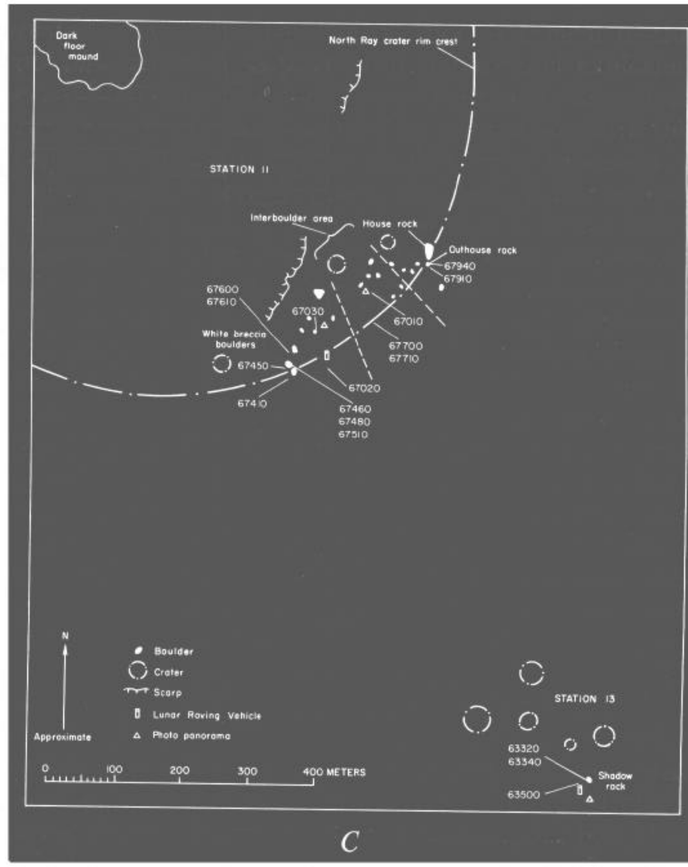

C

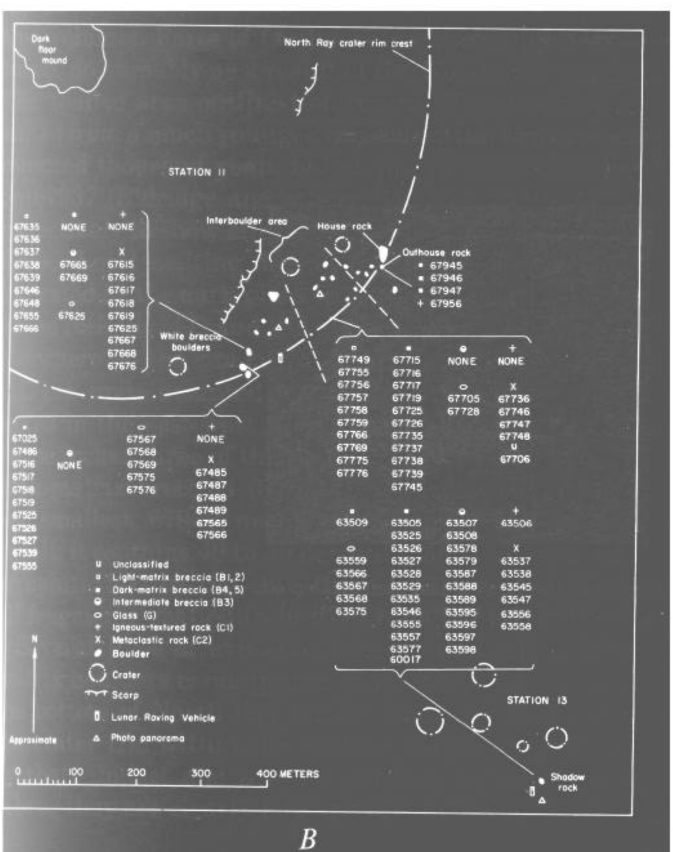

B

FIGURE 13.-Location of rocks and soils collected at stations 11 and 13. ***A,*** Rocks weighing more than 25 g. ***B,*** Rocks weighing 2 to 25 g. ***C***, Soil samples weigh more than 26 g.

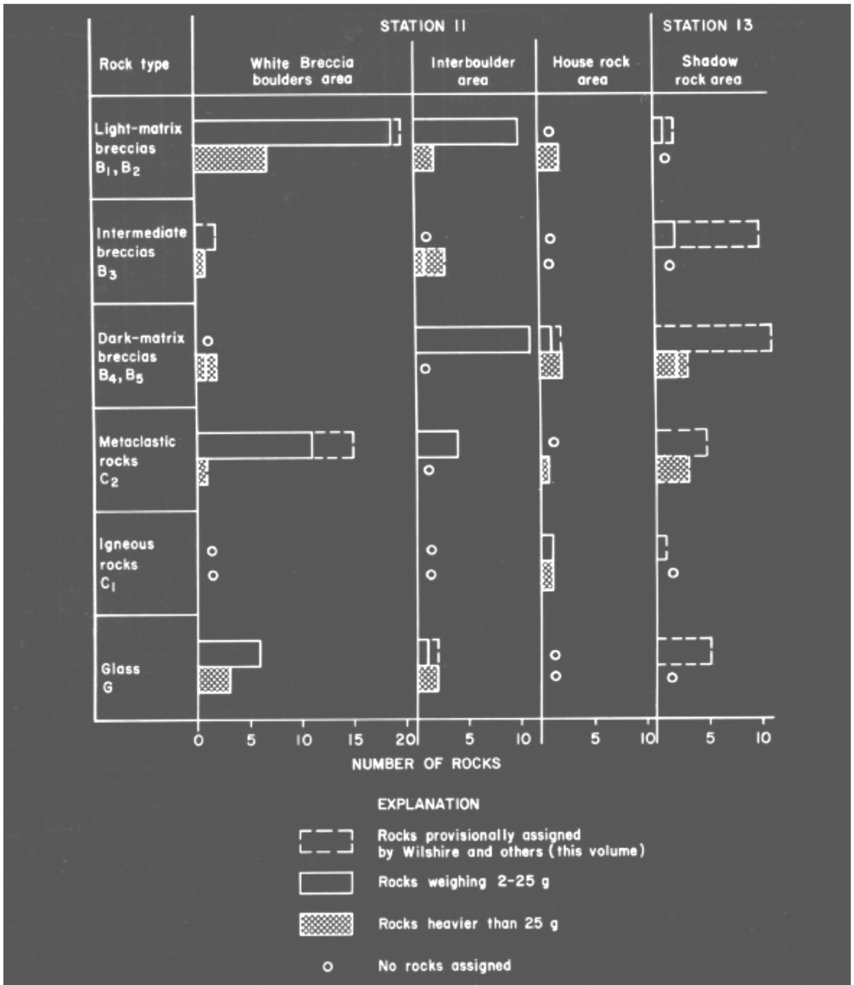

FIGURE 14.—Abundance of rock types collected from four localities at North Ray crater.

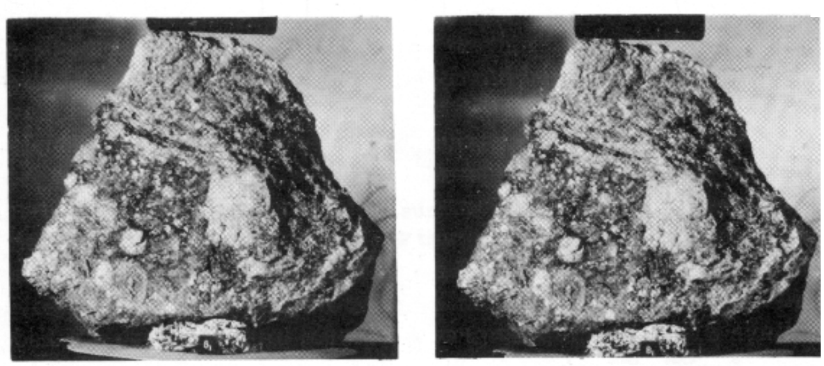

FIGURE 15.—Sample 67915, a dark-matrix breccia, the largest fragment collected from Outhouse rock. Scale in centimeters. NASA S–72–43917 and 43917B.

Six samples larger than 25 g were collected from the east face of Outhouse rock (table 2). The largest, 67915, is probably most representative of both large boulders (fig. 15), and its exact position on Outhouse rock is known (Sutton, this volume). It is a dark-matrix breccia containing a wide variety of clasts (Roeder and Weiblen, 1974a). Two plateau ages for 67915 determined by the ^{40}Ar-^{39}Ar method, 3.91 ± 0.05 and 3.99 ± 0.05 b.y. (Kirsten and others, 1973, p. 1760 and 1762), are considered to have selenochronologic significance. The lower age was determined on an anorthosite clast, the higher age from the matrix. The precision indicates that an age of about 3.95 b.y. for both samples is likely.

Other fragments collected from the face of Outhouse rock are mainly dark-matrix breccias and coherent metaclastic and igneous rocks (B4, B_5, C_2, and C_1 of Wilshire and others, this volume), a common lithologic association. One exception was a clast of light-matrix breccia, 67955 (fig. 16), selected for its unshocked appearance from the edge of an impact-spalled area (fig. 17), where the face of Outhouse rock had been struck by a high-velocity projectile. Other types of clasts within the boulder are represented by 67935 (fig. 18) and 67937 (fig. 19), metaclastic (C_2) rocks. A third type of clast, 67956 (fig. 20), is an igneous (C_1) rock having a subophitic texture much like that of 68415 (see Reed, fig. 9B, this volume) and 65055 (see Sanchez, fig. 20, this volume). Parts of Outhouse rock are highly fractured, presumably as a result of the North Ray impact. The spalled area outlined on figure 17 apparently resulted from a much younger impact within the past few hundred thousand years based on ^{26}Al measurements on 67937 (Eldridge and others, 1973, p. 2119). Other rocks likely to show effects of this event are 67935 and 67936. Local melting during the North Ray event is indicated by the dark glass splashes on the face of Outhouse rock (fig. 17) and the glass coating on fragments elsewhere on the rim crest.

Loose undocumented fragments and soil were collected in the east-west split between House and Outhouse rocks. Three of the four small rocks collected are dark-matrix breccias (67945-47, fig. 21). The fourth and smallest, 67948, may be a relict inclusion of mare basalt; it contains 40 to 50 percent mafic minerals with an ophitic texture (fig. 22). These rocks are most likely all fragments spalled from the large boulders.

Several lines of evidence suggest that these dark-matrix boulders came from a lower horizon near or at the bottom of North Ray crater. They are perched on the crater rim within the shallow depressions formed by their impact and are not overlain by subsequent debris; they are clearly late arrivals in the sequence of crater ejecta. This perched position is typical of the deepest material in terrestrial impact and explosion craters. In size and color, the rocks resemble the coarse rubble on the crater floor and, by comparison with the central mounds in nearby craters, may represent a more resistant stratum near the floor of the craters (Hodges, 1972a; Ulrich and Reed, this volume). Dark rocks are sparse on the crater rim crest (10-30 percent, fig. 12). The more abundant light-matrix breccias here and radially away from the rim probably represent shallower materials overlying the dark-matrix rocks in the crater wall. The large 10-m blocks in the northeast wall of the crater appear in telephotographs to be light-matrix breccias (fig. 23, and pl. 9, pan 36) with some degree of lateral continuity, suggesting at least a crude stratigraphic relation to the materials above and below. The slightly convex shape of the crater wall as seen from the southeast rim (fig. 4) indicates that relatively softer, less coherent materials in the upper wall overlie more resistant material at depth.

WHITE BRECCIA BOULDERS

A group of rounded light-colored boulders was another major sampling target at the rim of North Ray, about 50 m west of the LRV parking spot. The sampling done in the vicinity of the LRV was within this area, and the largest number of samples from station 11 was collected at this westernmost location, as shown in figure 13. The classification and geologic significance of all the rocks weighing more than 2 g (figs. 13A, B) are given in table 3.

The most distinctive characteristics of the rocks here are the well-rounded profiles, deeply filleted margins, and light-gray to white color (fig. 10). The lengths of the largest boulders are about four times their height. The returned samples typically are light-matrix breccias, which are generally very friable and contain coherent clasts of dark-matrix breccia (fig. 11). The rock probably most representative of these boulders is sample 67455 (fig. 24), collected from several loose fragments on top of a boulder approximately 6 m long and 1.5 m high (figs. 10 and 25A). A light-colored clast from this sample has a plateau age of 3.91 ± 0.12 b.y. determined by the ^{40}Ar-^{39}Ar method (Kirsten and others, 1973, p. 1762), essentially the same as the age of 67915 from Outhouse rock. This rock, like many of the rocks of this group, crumbles so badly that it is impossible to reconstruct its lunar orientation. The friable texture is expressed microscopically by extensive irregular fracturing through the matrix and around the more coherent clasts (fig. 25B), referred to as glass selvages by Wilshire and others (this volume, fig. 4A).

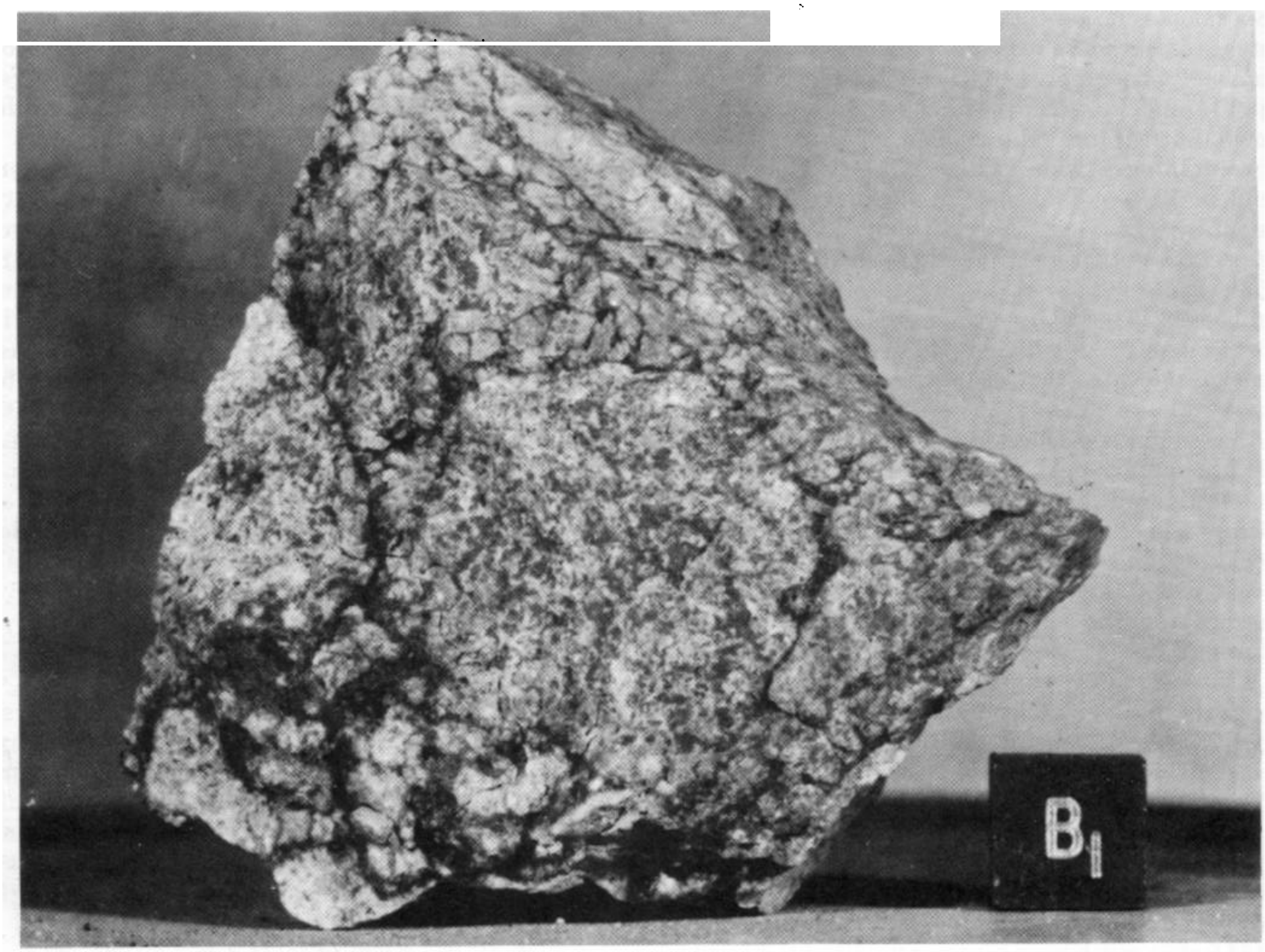

Figure 16.-Sample 67955, a clast of light-matrix breccia from Outhouse rock. Cube is 1 cm. NASA S-72-45681.

FIGURE 17.-Impact-spalled area on east face of Outhouse rock. AS16-106-17345.

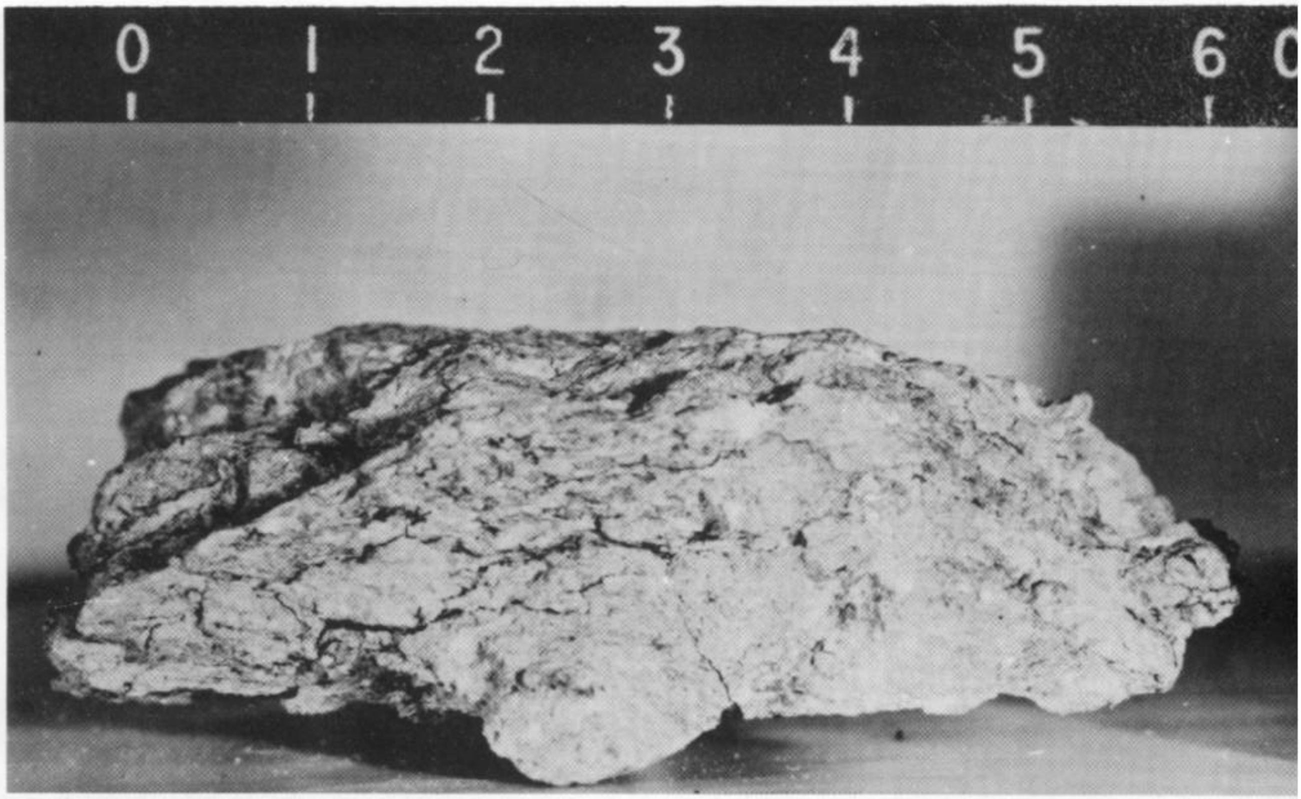

FIGURE 18.-Sample 67935, a metaclastic rock broken off the east face of Outhouse rock. NASA S-72-37784.

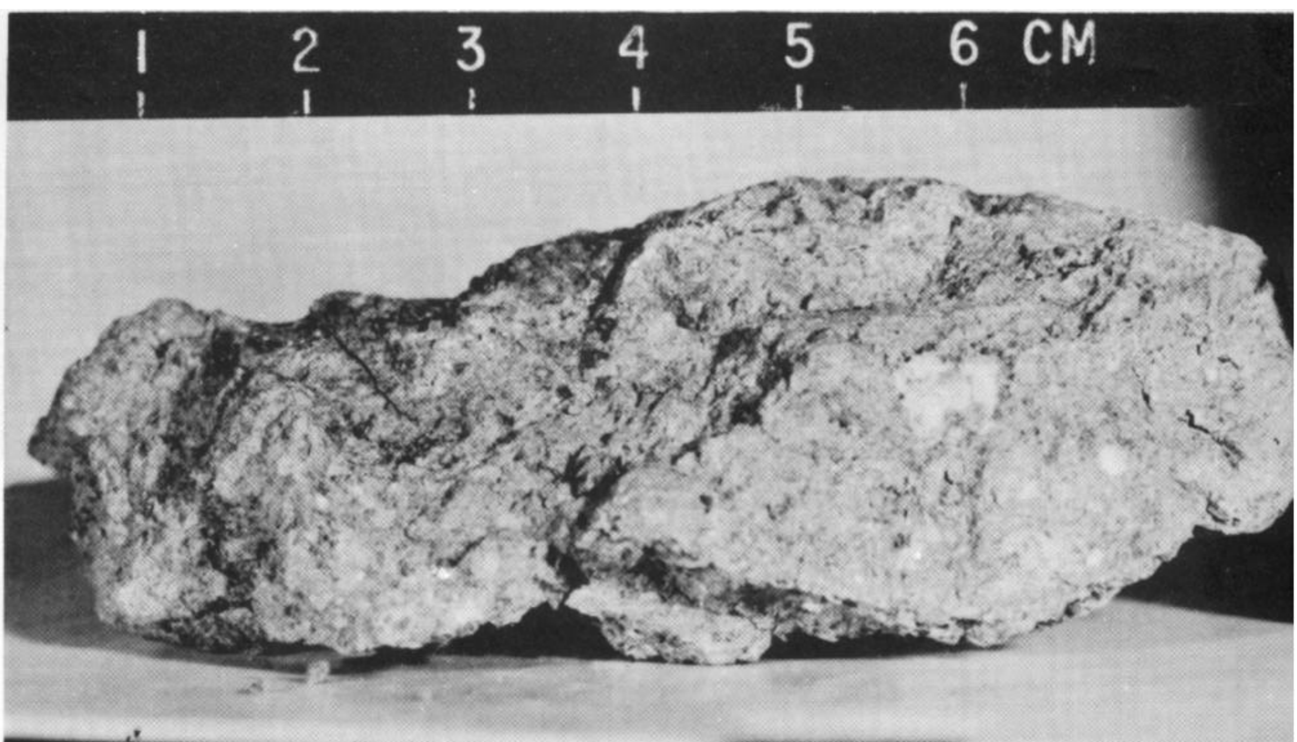

Figure 19.-Sample 67937, a metaclastic rock from Outhouse rock. NASA

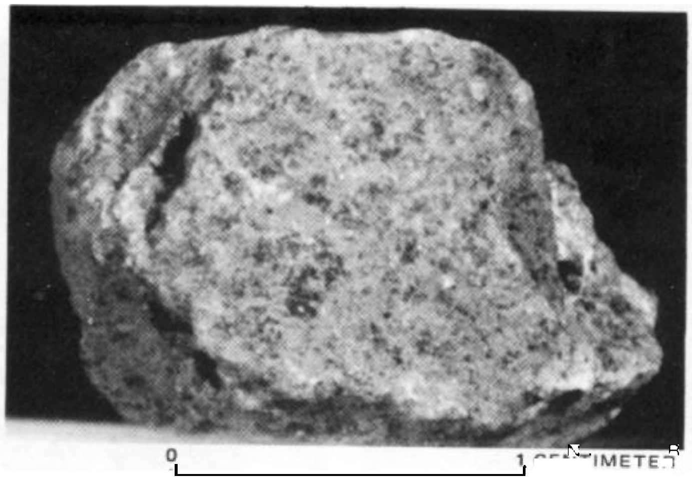

FIGURE 20.-Sample 67956, a rock with igneous texture from Outhouse rock. NASA S-72-37547.

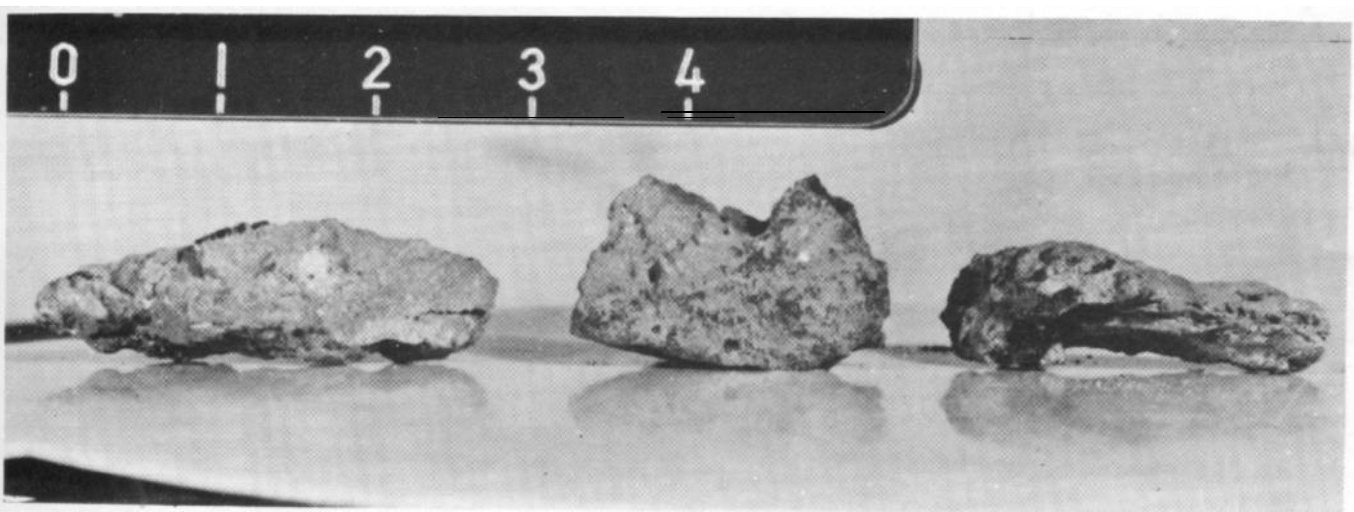

FIGURE 21.-Three dark-matrix breccias collected from the east-west split between House and Outhouse rocks; left to right, 67945, 67946, 67947. Scale in centimeters. NASA

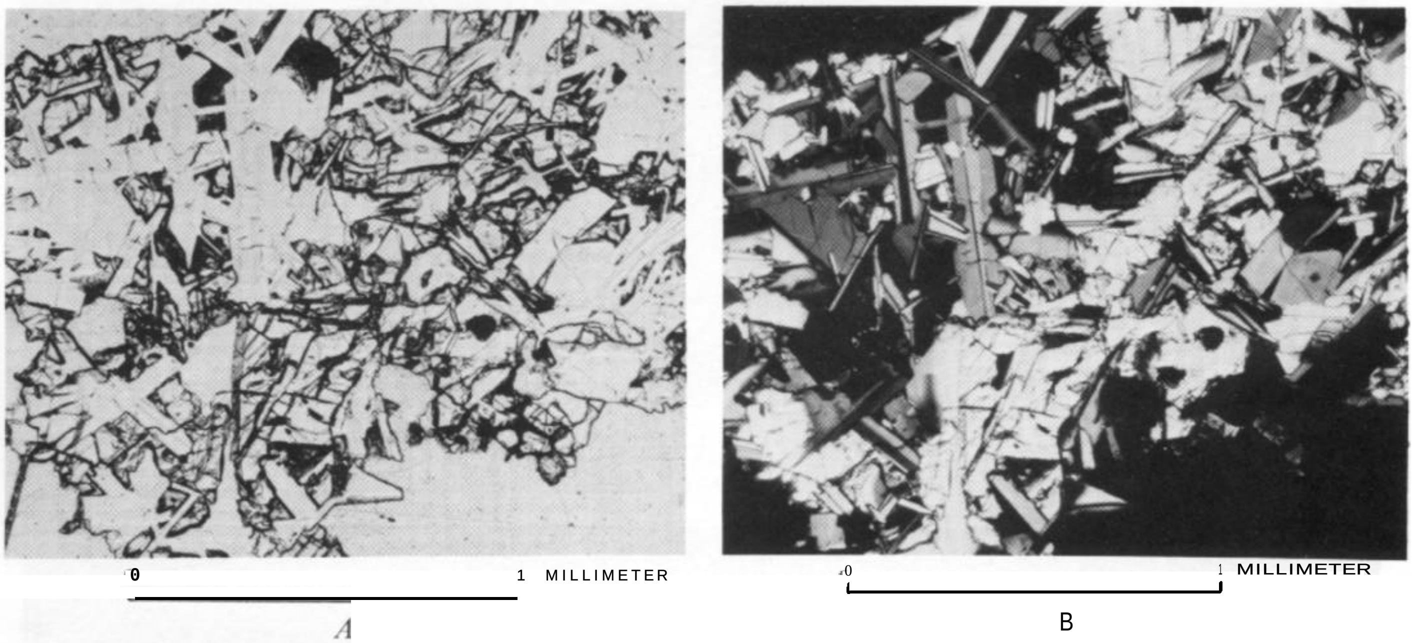

FIGURE 22.-Ophitic fragment 67948 (1.59 g) collected from the east-west split between House and Outhouse rocks. A, Photomicrograph of 67948, 15 showing pyroxene (high relief) and plagioclase laths. Plane-polarized light. B. Same .samples as A, cross-polarized light.

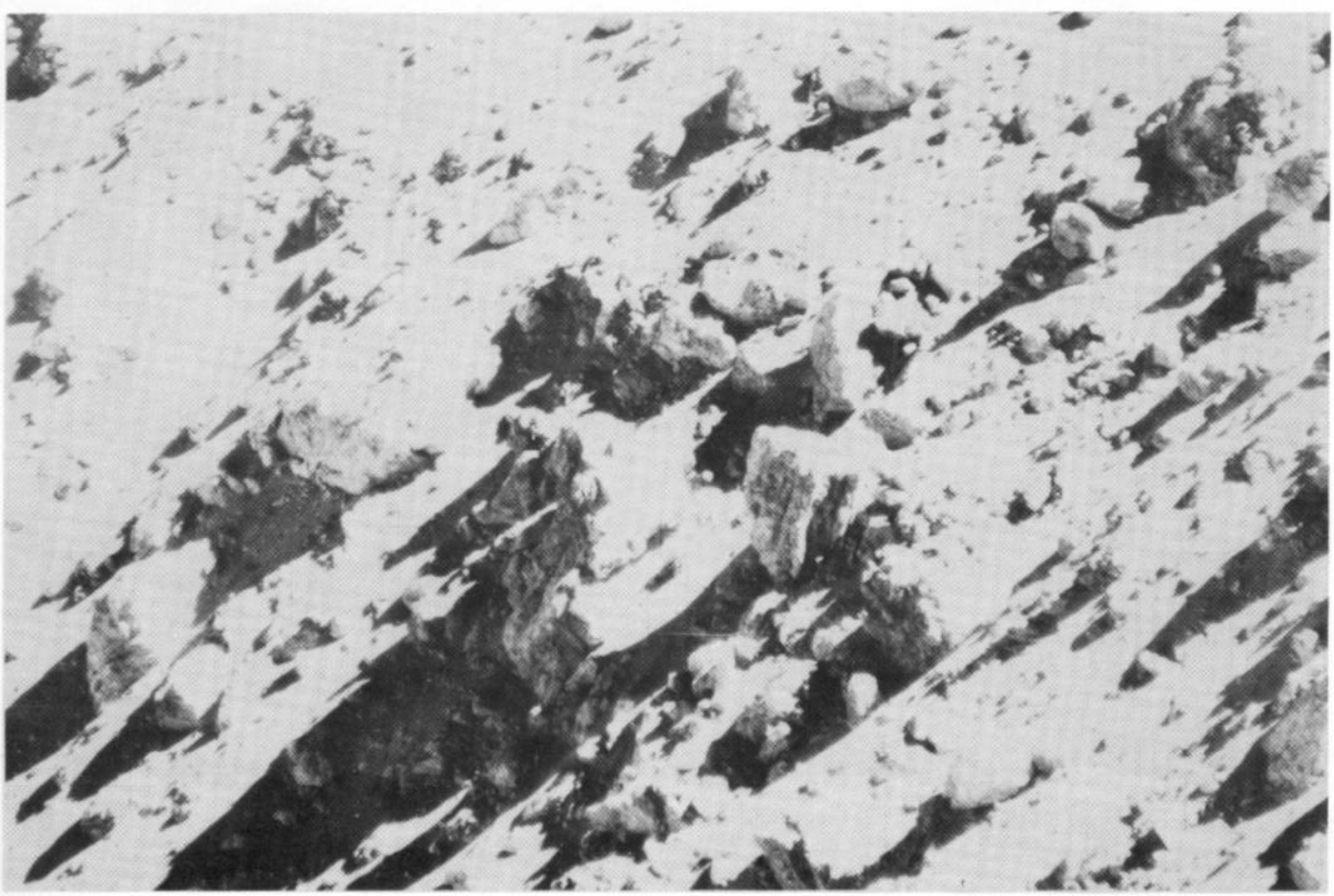

FIGURE 23.-Telephotograph of large light-matrix breccia blocks on northeast wall of North Ray crater. Intentionally underexposed to enhance textures in shadows. From AFGIT (1973). Reprinted with permission of the American Association for the Advancement of Science.

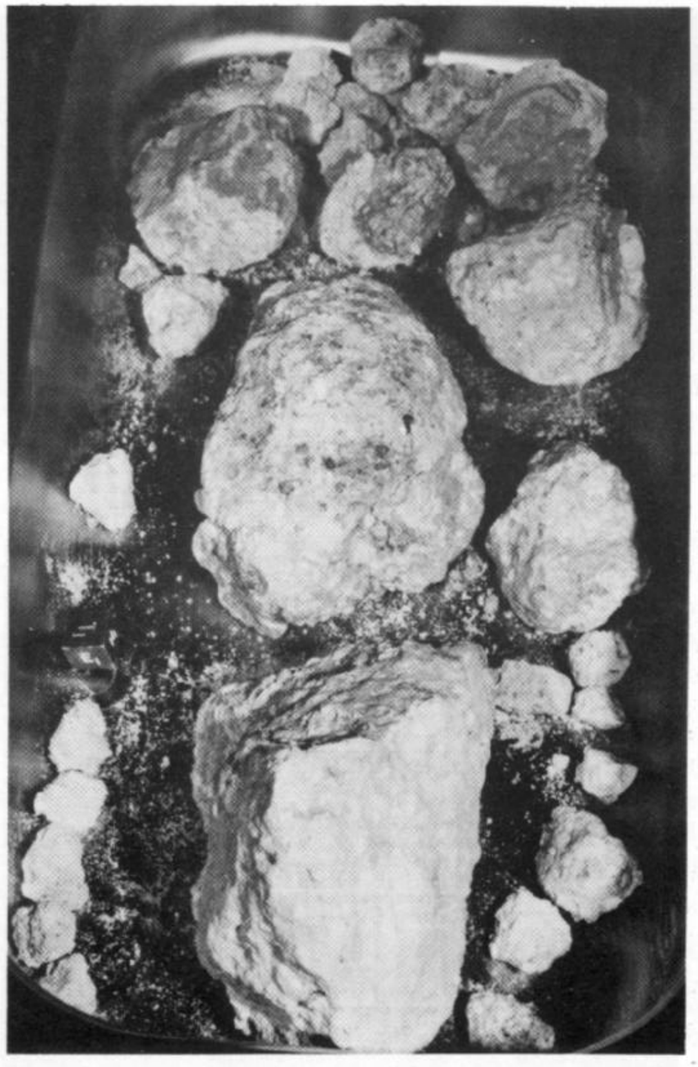

Figure 24.-Broken fragments and fines of sample 67455, a light-matrix breccla collected from the top of a White breccia boulder illustrated in figures 10 and 254. Note few small dark clasts. NASA S-72-38194. Cube is 1 cm.

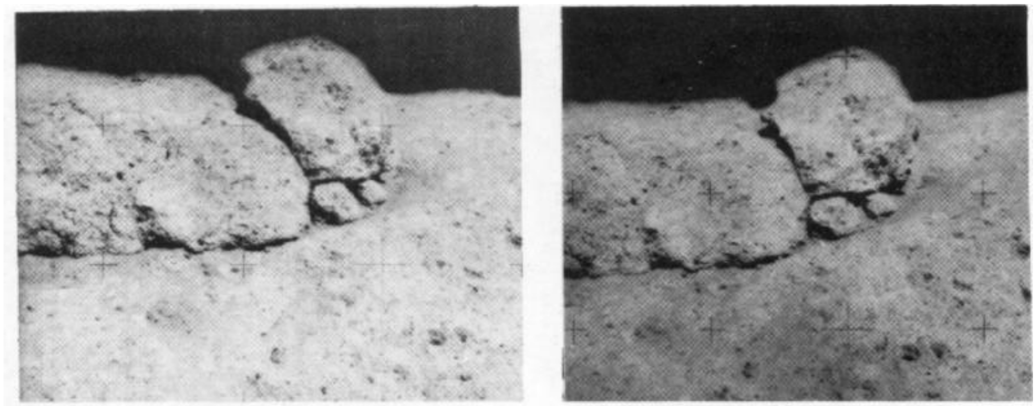

A

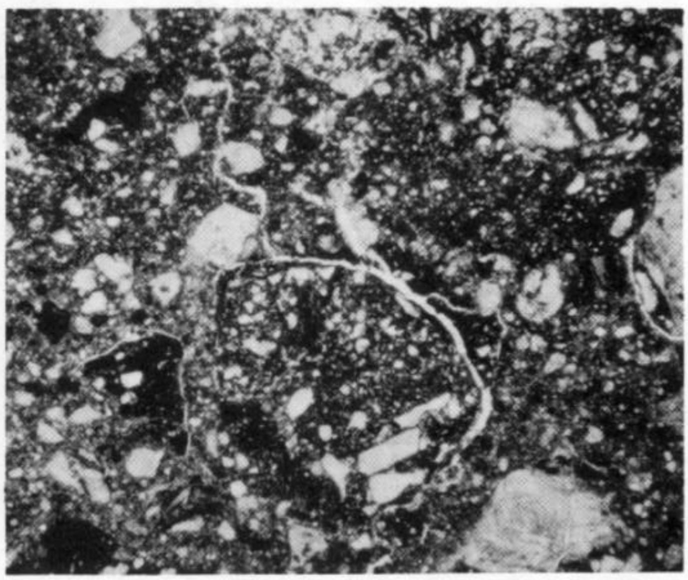

B

FIGURE 25.--Sample 67455. ***A,*** Stereopair of the top of a White breccia boulder and the fragments of sample 67455 before sampling. AS16-106-17331 17332. ***B.*** Photomicrograph of 67455, 57 illustrating irregular fractures that penetrate the matrix of shocked feldspar grains but avoid dark-matrix Plane-polarized light.

The rapid mechanical breakdown of these rocks relative to the dark-matrix boulders may be explained by a combination of thermal cycling, which doubtless causes unequal expansion of the dark clasts and light matrix, and micrometeorite bombardment of the surface whereby the rock disintegrates along the irregular fractures and the more coherent fragments collected in the rake samples are preferentially preserved. These processes do not appear to be as effective in the dark-matrix boulders.

A dark-matrix breccia clast (67475) collected from the same boulder as 67455 illustrates very well the criteria by which some clasts can be identified, even when separated from their host. Three views of 67475 (fig. 26) show the weathered surface, a fresh dark-matrix surface, and a surface coated with the feldspathic host material. Fragment 67718 from a rake sample in the Interboulder area is another specimen whose surfaces reveal its relation to the host (see Smith and Steele, 1972, p. 81).

Other samples in the White breccia boulder area that exceed 100 g in weight and probably represent the majority of rocks there are shown in figure 27. The only crystalline rocks recognized by Wilshire and others (this volume) are 16 rake samples classified as metaclastic (C_2); all but one of these weigh less than 25 g. Their occurrence as smaller rocks suggests only that they are residual coherent clasts “weathered” out of the local boulders. Two examples of such clasts within light-matrix breccias are 67415 and 67455 (fig. 28).

One rock, 67215 (also weighing more than 100 g), was collected because of its unabraded rock surface. It is described by Horz and others (1972, p. 7-25) as a moderately tough breccia. This rock has not been studied (as of this writing).

INTERBOULDER AREA

Approximately midway between the White breccia boulders and House rock is a sampling area chosen because it was relatively free of large rocks (fig. 13). From this location, a third photographic survey (east panorama, pl. 9, pan 20; and fig. 4) was taken of the far crater wall. (Table 4 and figs. 13A, B, and *29A-E* show the types of breccias collected in this area.) Light-matrix breccias, typified by 67055 and 67075 (fig. *29B, C*), are abundant but not as predominant as in the White breccia boulder area. The appearance of sample 67075 in this section is typical of a crushed anorthosite (B_1) breccia (fig. 30). Samples 67015 and 67115 (fig. 30A, *E*), assigned to the intermediate B_3 class by Wilshire and others (this volume) are considered here to be light-matrix breccias because of their matrix color and friable textures. The one dark-matrix fragment collected (67718, 49 g) is covered with white material (Smith and Steele, 1972, p. 82-l) indicative of its former location within a light-matrix host. Rock 67095 (fig. 29D), glass-coated and cemented, is a good example of the glass of class G of Wilshire and others (this volume). Astronaut Young associated it with a l-m secondary crater on the North Ray rim; it may be an exotic arrival postdating the North Ray event or, alternatively, a fragment of late-stage melt from North Ray.

Fragments weighing less than 25 g and collected in the Interboulder area (see figs. 13B, 14) reflect a concentration of intermediate-gray-matrix breccias (B_3) collected mainly in the rake sample (67715-67776). This breccia class appears to be transitional between the light- and dark-matrix breccias and is most commonly listed with light-matrix breccias as an alternative designation by Wilshire and others (this volume). Its origin may be considered similar to that of the light-mat&ix breccias, with some enrichment in the dark glass components. Consequently, a selective concentration of more resistant clasts of B_3 material occurs as residuum from an inferred light-matrix (B, and B_2) host rock. Rock 67235, like 67215 from the White breccia boulder area, has not been studied as of this writing but is described by Horz and others (1972, p. 7-25) as a hard recrystallized breccia in appearance.

SHADOW ROCK’AREA

Station 13 was planned for the outer edge of the continuous ejecta blanket of North Ray crater. The objective was to collect a radial sample in the region where the shallowest stratigraphic material would be present. As the outer edge of the ejecta blanket was not identifiable, the astronauts selected a location in the vicinity of several large boulders described while enroute to the crater rim crest.

The primary source of rock samples greater than 25 g was the single large boulder named Shadow rock, about 5 m long and about 4 m high. It has a distinct moat around its base (fig. 9), presumably part of a shallow secondary crater created by impact of the boulder when ejected from North Ray crater. No.fillet of material was shed from its surface. Its shape and apparent resistance to erosion suggest that it is similar to the dark-matrix breccias in the House rock area. And its color and texture are typical of dark-matrix rocks (illustrated close-up in figure 31).

Of the rock samplescollected at station 13, (table 5) only one, 60017, weighs more than 100 g (fig. 32). It is very dark, fine grained, and vesicular and apparently has a high percentage of glass in its matrix. Prominent elongate vugs or vesicle pipes were noted by Astronaut

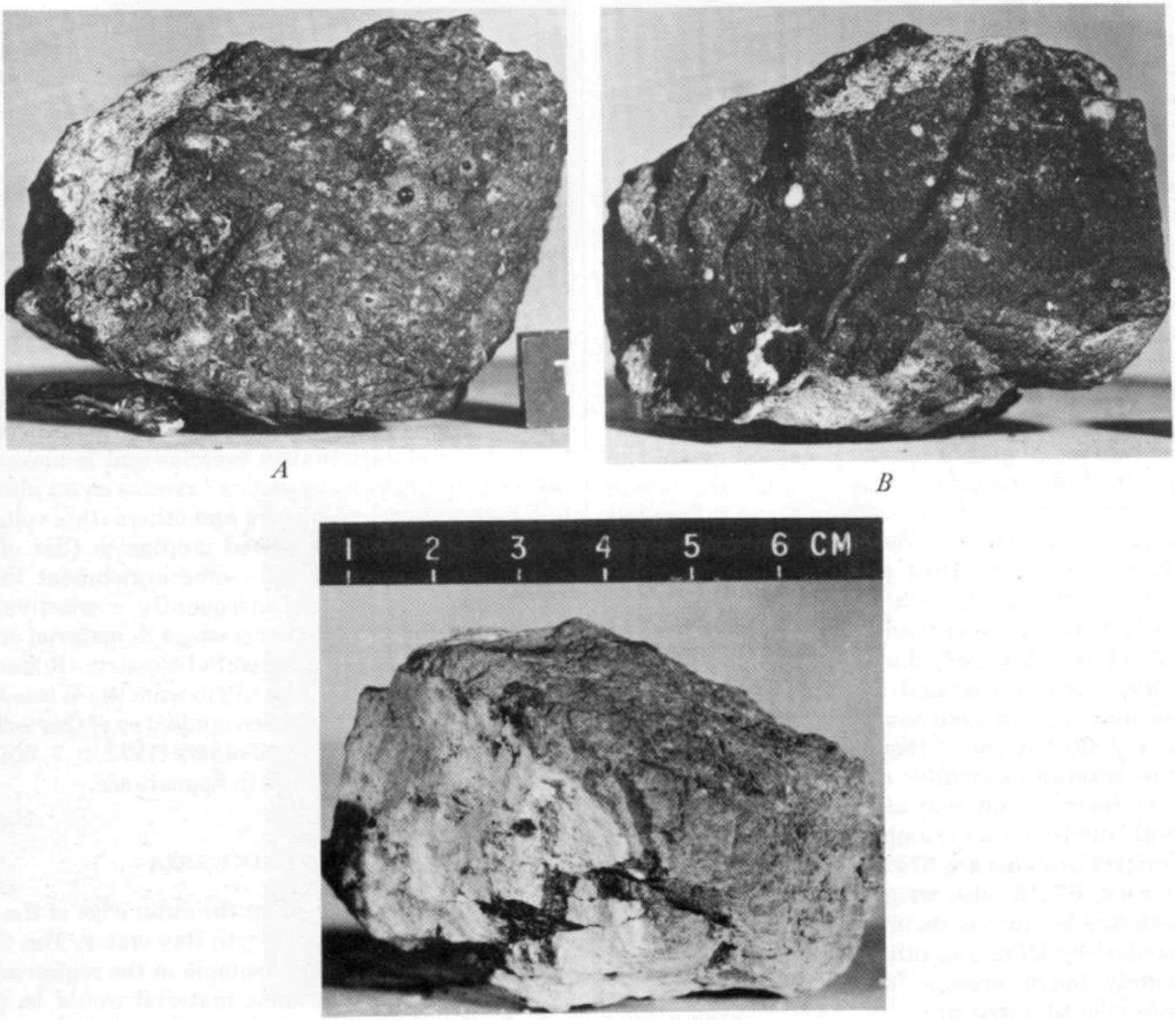

A *B*

C

Figure 26.-Sample 67475, a dark-matrix clast from the White breccia boulder of 67455. ***A,*** Weathered surface with glass-lined zap pits (NASA S-72-43359). ***B,*** Fresh broken surface showing white feldspathic clasts (NASA S-72-43363). C, Broken surface showing coating of light feldspathic matrix of host material (NASA S-72-37958).

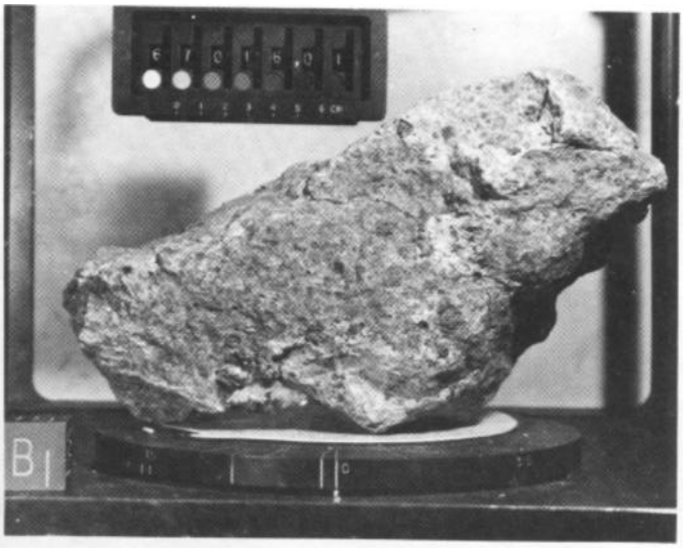

A

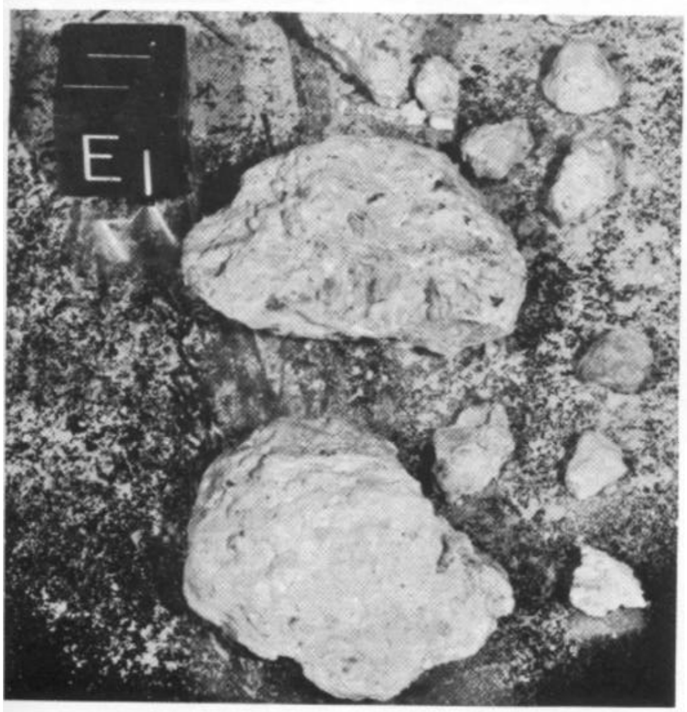

B

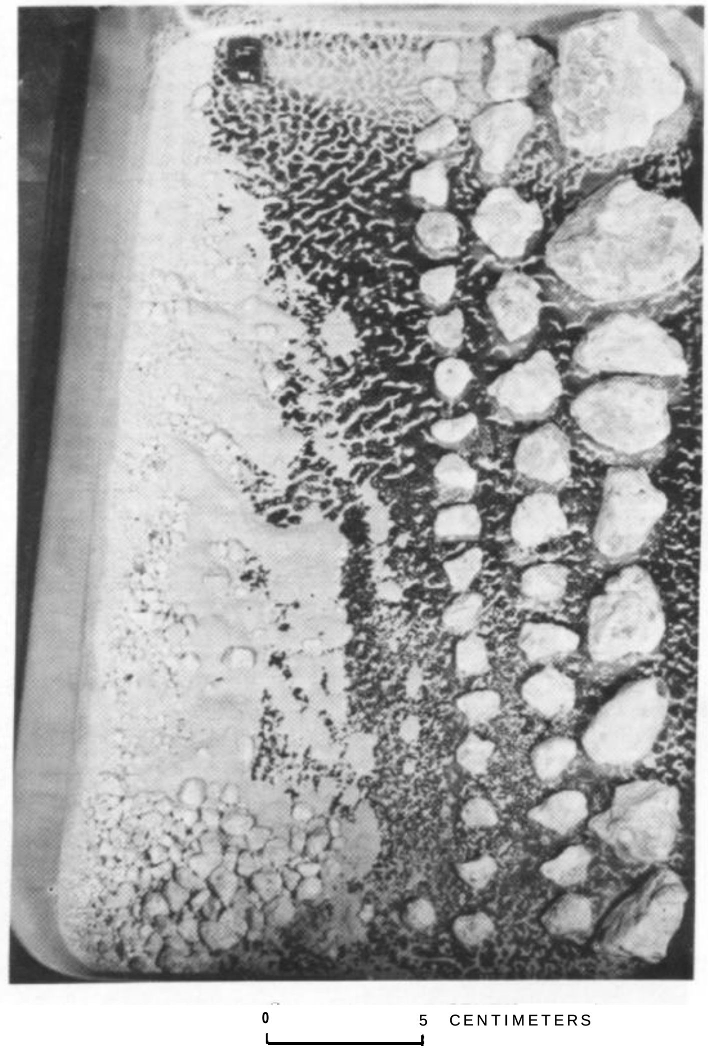

C

FIGURE 27.-Several rocks heavier than 100 g collected in the White breccia boulder area. A, Part of 67016, intermediate-gray matrix (B_3 of Wilshire and others, this volume\. S-72-39230. B. 67035, light-matrix (B_2) broken in transit, S-72-37542. C, 67415, light-matrix (B_1) broken in transit, S-72-39038. D, 67435. half light, half dark. (B_4 of Wilshire and thin volume). S-72-43897 stereopair.

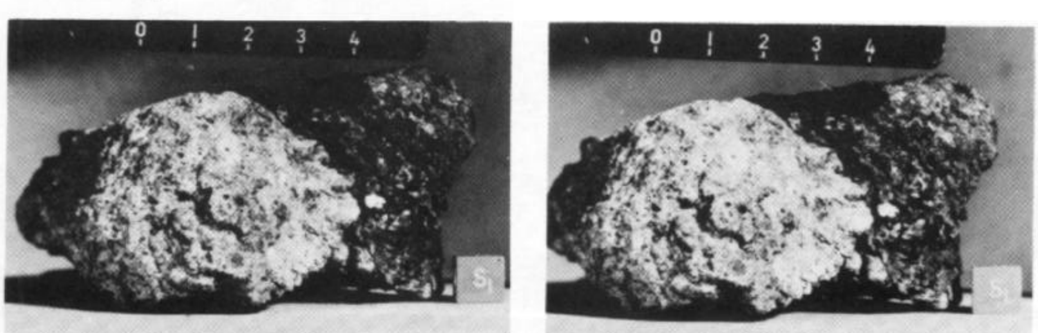

D

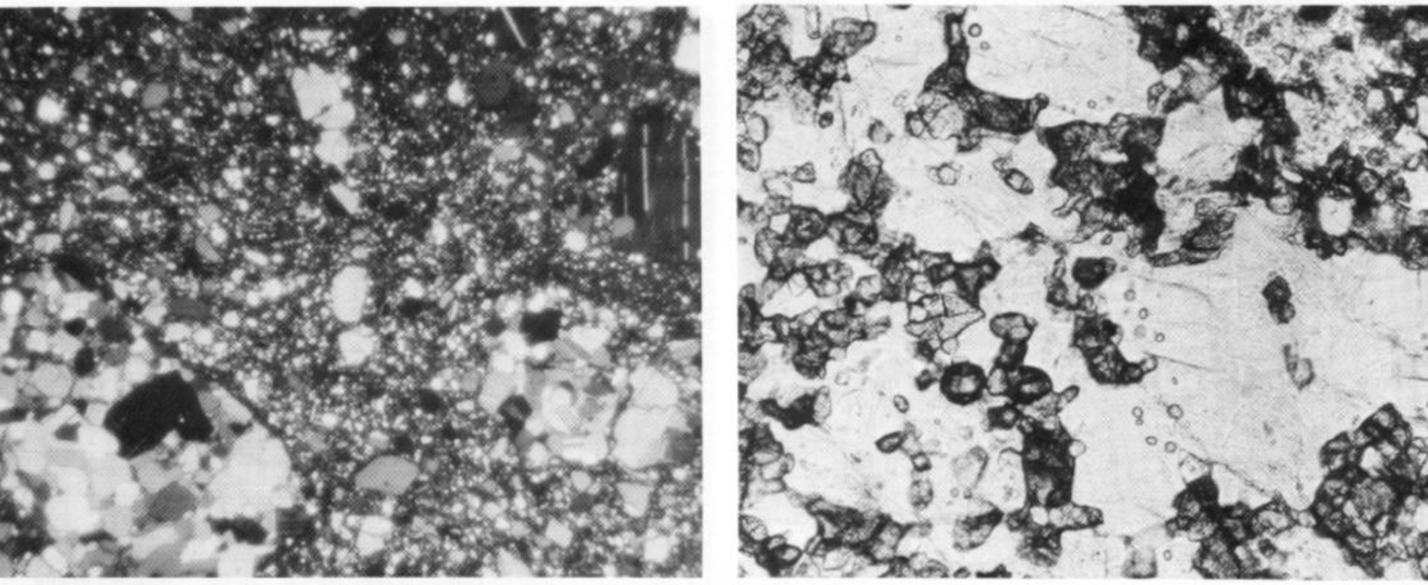

FIGURE 28.-Photomicrographs of metamorphic clasts within light-matrix breccias. *A*, Granoblastic plagioclase clast in matrix consisting predominantly of crushed feldspar: 67415,14: cross-polarized light. *B*, Poikiloblastic plagioclase enclosing mafic minerals: 67465,57; light.

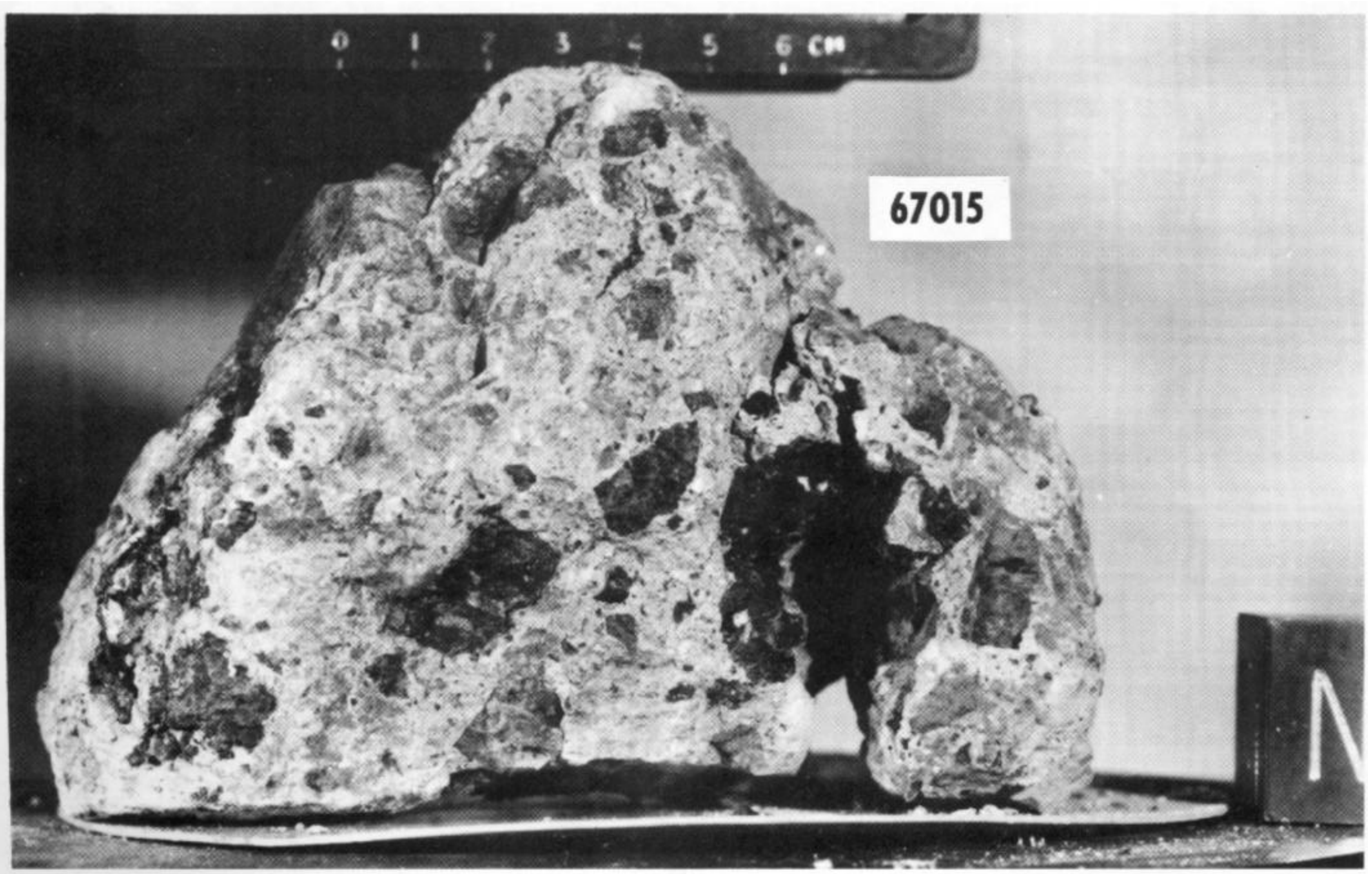

A

29.-Caption on facing page.

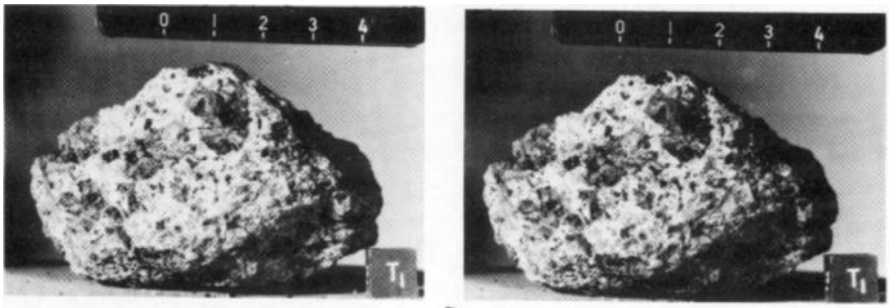

B

C

FIGURE 29.-Rocks heavier than 100 g collected from the Interboulder area. *A, 67015,* light-matrix (B_3 of Wilshire and others), S-72-37216. B, 67055, light-matrix (B_2), S 72-43880 stercopair. C, 67075,light-matrix (B_1), S-72-37539. D, 67095, glass coated (G), S-72-43076 stereopair. E, 67115, light-matrix (B_3 of Wilshire and others), ,S72-37718.

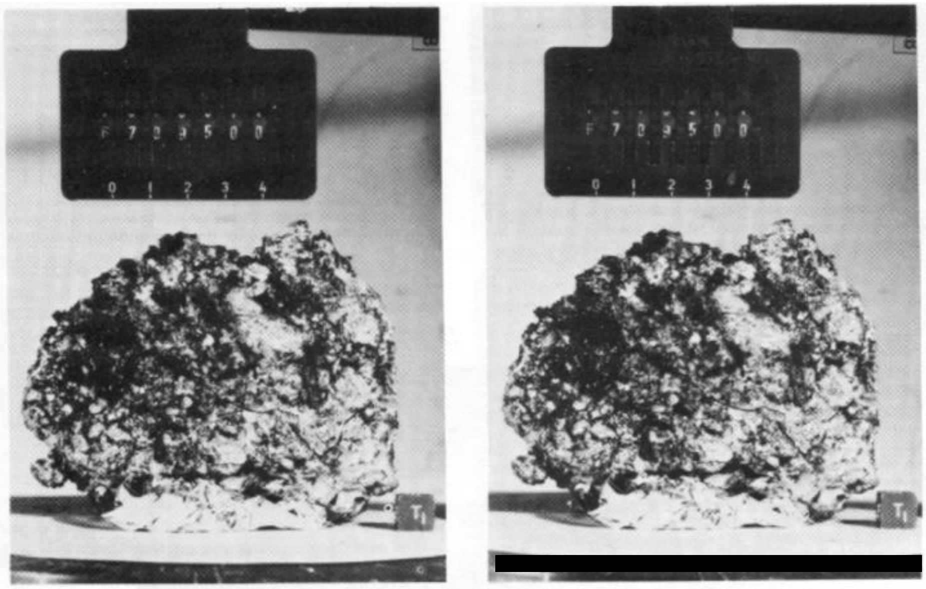

D

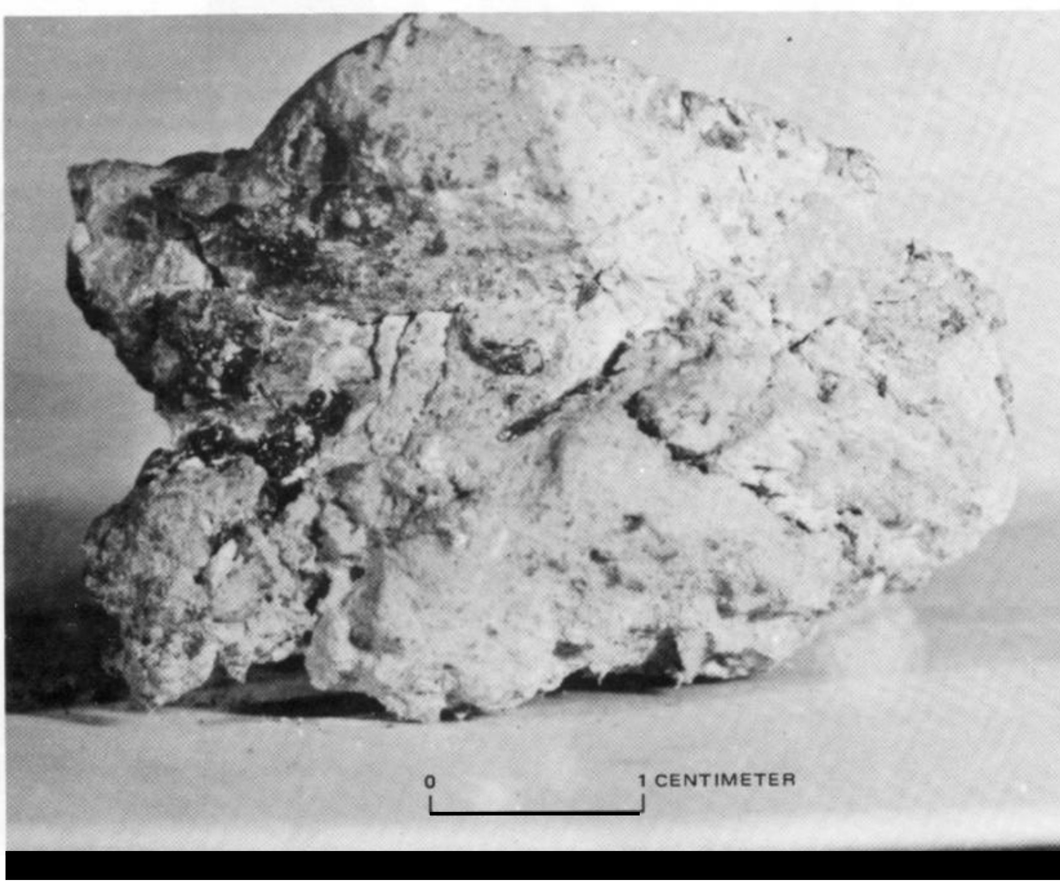

E

FIGURE 29.-Caption on preceding page.

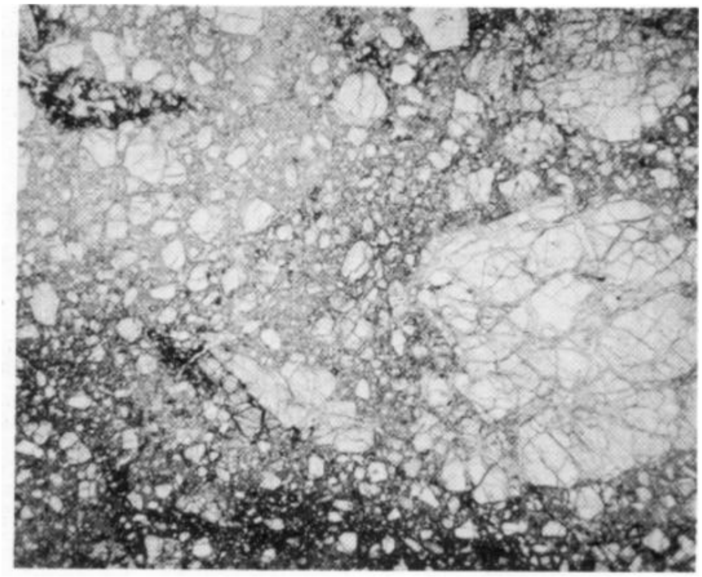

0 1 MILLIMETER

A

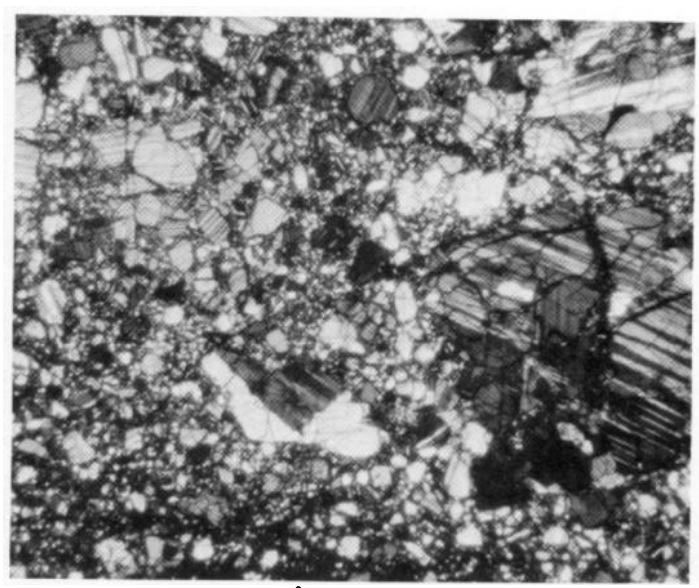

0 1 MILLIMETER

B

FIGURE 30.-Photomicrographs of a typical light-matrix hreccia from the Interboulder area. *A*, Plane-polarized light. B, Cross-polarized light. Glass occurs as veinlets within larger plagioclase clasts and in fine-grained matrix.

FIGURE :31.-Surface texture of Shadow rock. Closeup of overhanging southwest corner (arrow). AS16–106–17410; inset photograph AS16- 106- 17393: view is northeast.

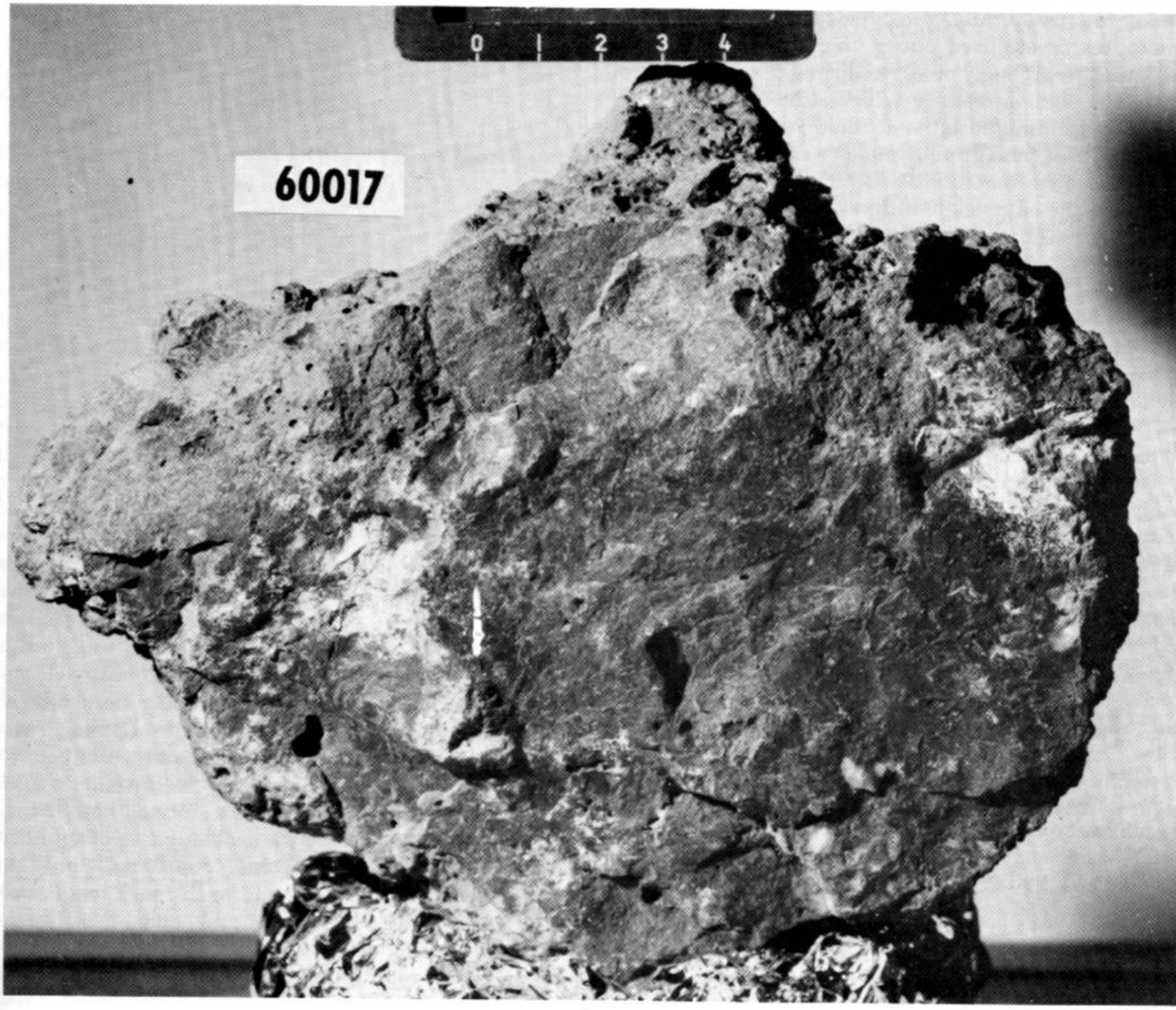

FIGURE 32.-Dark-matrix breccia, 60017, (B_4) from near Shadow rock. Scale in centimeters. NASA S-72-36943.

Duke. Microscopically, it can be seen that plagioclase microlites crystallized out of the glassy matrix and vesiculation probably occurred during the quenching of the glass; some late-stage vesiculation is indicated by abruptly terminated laths at some vesicle boundaries (fig. 33). The remaining samples weighing more than 25 g are dark-matrix (B_4, B_5) and metaclastic (C_2) rocks. Of the samples less than 25 g, a large number (nine) are tentatively classified as intermediate-gray-matrix breccias (B_3) (Wilshire and others, this volume); 11 are dark-matrix breccias (fig. 14). Metaclastic and glassy rocks collected in the rake sample, 5 to 10 m west of Shadow rock, probably represent rocks high in the North Ray walls. Removal from these assignments of samples of uncertain classification (fig. 14) leaves few samples that can be interpreted with confidence.

The most significant rocks, then, are the largest samples derived from a known local source, Shadow rock. Like House rock and Outhouse rock, Shadow rock must have been derived from North Ray crater and deposited late in the ejecta sequence; otherwise later deposits would have banked against its northwestern side. Whereas most of the local blocks are light colored (fig. 12), Shadow rock belongs to a small group of dark rocks that are larger and more angular than most of the fragments (about 20 percent of all the blocks in view). It is probably part of a,discontinuous ray of dark resistant breccias from a deep unit that is overlain by light-matrix rocks in North Ray crater.

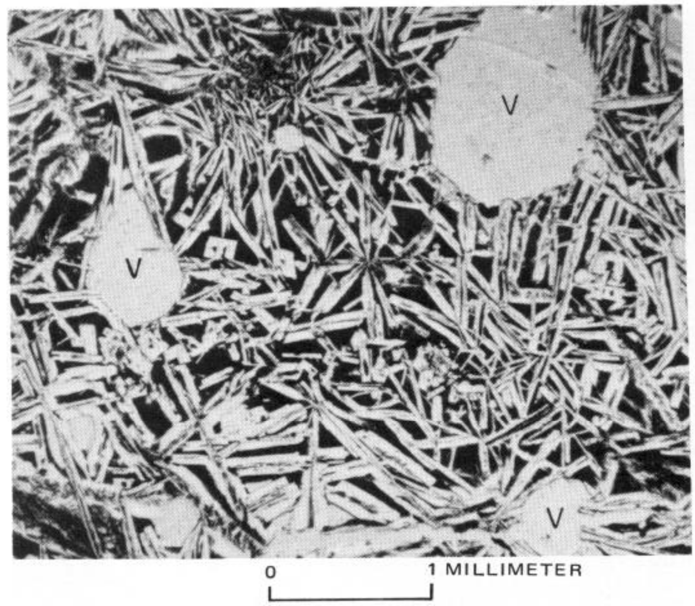

FIGURE 33.-Photomicrograph of 60017, 112, showing vesicles (V) that both conform to and crosscut plagioclase quench crystals in glassy dark-matrix breccia. Plane-polarized light.

NORTH RAY SOILS

The soils on the rim of North Ray crater are distinct from those at other sampling stations within the traverse area in that they are generally very thin and light in color. They are similar to one another in modal and chemical composition (Heiken and others, 1973, p. 261-263). Light-matrix breccias are especially abundant in .these soils (approximately 40 percent, G. J. Taylor and others, 1973, fig. 8).

The soils at each of the sampling localities (table 6) were described by the astronauts. At the White breccia boulders, where large fillets occur around the very friable rocks, Duke commented, “The regolith here * * * on this crater rim is really soft. We’re sinking in on the slopes about six inches or so” (see fig. 10). Elsewhere it was a centimeter or less as indicated by the bootprints in the station 11 panorama (pl. 8, pan 18). At the Interboulder area, illustrated in the foreground of figure 4, descriptions were, “Right under the upper dull-gray soil there’s a layer of whitish material, much like it was at South Ray” and “It’s hard under there * * * there must be a big rock under here. I can’t get the rake in * * * It’s all white under here. Down about a centimeter or less, it’s all white” (Duke). This color difference, gray on the surface and white below, was also described near Shadow rock (station 13) and everywhere else at the site except stations LM, 8, and 9. It is probably caused by the accumulation of agglutinates at the surface (Adams and McCord, 1973, p. 171), a process that may also account for the dark tongues of surface debris seen draping the upper wall of North Ray in figure 3. The lighter areas between these tongues may represent more active soil movement downslope, where darker soils have slid away. Low scarps commonly border the more stable gray slopes, and a few boulder tracks are present where larger fragments have rolled or slid downward.

The agglutinate contents of the darker soils, much lower than elsewhere in the traverse area, indicate a lack of maturity and thus the low relative age of North Ray soils (McKay and Heiken, 1973, p. 42). Exposure ages have been reported as 30 to 60 m.y. (Schaeffer and Husain, 1973, p. 1858; Kirsten and others, 1973, p. 1775; Turner and others, 1973, p. 1903; Marti and others, 1973, p. 2039).

At House rock, Duke, while attempting to sample the east-west split (fig. 8), reported, “This soil here is very hard and the rake really won’t go into it. It’s bending tines * * *. The purpose of sampling in the west-trending opening was to obtain materials (soil 67940) shielded from the solar wind and to identify, by comparison with a nearby reference soil sample (67960), the components concentrated or redistributed by the solar wind. No chemical or modal differences are found in these soils (Heiken and others, 1973, p. 262); only minor contributions of soil-size particles spalled from the adjacent boulders are recognized. Adams and McCord (1973, fig. 4 and p. 170), however, found a lower reflectance for 67941’ when compared with 67461 from the White breccia boulder area, even though the agglutinate contents are the same (20 percent). They attribute the lower reflectance of the House rock soils to enrichment in dark-matrix breccia fragments.

At Shadow rock the astronauts collected a soil sample from beneath the overhang on the west end of the rock in the deepest recess (fig. 31). It was hoped that the sample had been permanently in shadow since the rock was emplaced, and the investigators intended to determine whether volatile elements had been concentrated in such a cold trap. The shadow at the time of sampling is shown in figure 34; the sun elevation angle was 46” above horizontal, its azimuth was 12” north of east. At sunrise and sunset, the maximum progression of the sun’s azimuth is 1” to 2” north of an east-west line. This and the estimated movement of sunlight into the shadowed area (shown on fig. 34) during a single lunation make it unlikely that any exposed soil remains permanently shadowed, despite Astronaut Duke’s observation that the shadowed area was downslope (beneath the rock). A second soil sample (63340) was collected from beneath the first and therefore was a buried soil rather than an exposed shadowed soil.

The North Ray soils have not been found to differ significantly in lithophile trace-element abundances; strontium contents are slightly higher in these soils than elsewhere, probably reflecting higher plagioclase contents in North Ray target materials (Philpott and others, 1973, p. 1433). North Ray rim soils (including 67941) exhibit no apparent differences in carbon content but as a group are significantly lower in carbon than all other Apollo 16 soils measured by Moore and others (1973, p. 1616). If carbon content is mainly a product of solar wind effects, the contribution on the rim of North Ray crater is relatively small and is the same for the east-west split as in unshielded areas.

The apparent meteoritic component in the North Ray soils is lower than elsewhere; this too is indicative of relative immaturity (see Freeman, this volume).

‘The fifth digit “1” in sample numbers denotes the sieve fraction of soil that is less than 1 mm.

GEOPHYSICS

Geophysical data in the North Ray area consist of a single three-vector reading on the Lunar Portable Magnetometer at station 13. The resultant magnetic anomaly reported was about 300 gammas, down and to the southwest, the largest recorded at this site and larger than any recorded at Apollo 14 or 15 sites (Dyal and others, 1972, p. 12-7). This and the readings from station 2 and in the LM area are interpreted by Strangway and others (1973, p. 113-114) as indicative of a breccia blanket of the order of 1 km thick under the Cayley plains. This blanket, by their hypothesis, was emplaced within a field of a few thousand gammas cooled from a temperature higher than 700°C, forming a moderately welded rock mass with a high remanent magnetization.

The only lunar rocks known at this time (1974) to have stable magnetization sufficient to fit this model are a moderately welded, dark-matrix soil breccia (15498) from Dune crater at the Hadley-Apennine (Apollo 15) site and an Apollo 11 chip from soil 10085 (Strangway and others, 1973, p. 113). As unwelded materials and (surprisingly) highly welded and igneous rocks do not carry strong remanent magnetizations, it is possible that the large magnetic fields required are produced by local or regional impact events (such as 10-km or larger craters) wherein only the melted and rapidly cooled breccias retain the transient fields. The igneous-textured rocks cooled slowly enough that the short-lived impact-induced fields had disappeared by the time they passed through the Curie point. The melt-poor light-matrix breccias, never hot enough to pass through the Curie point, therefore were not magnetized.

SUMMARY

North Ray crater proved to be an excellent source for a large variety of samples and photographs representing the best available documentation for stratigraphic interpretations anywhere in the Apollo 16 traverse area. The rounded form of the crater rim and the convex shape of its generally smooth walls indicate a target material of relatively low strength.

Rocks on the rim and wall of North Ray crater are mainly of two types: light-matrix and dark-matrix feldspathic breccias with clasts and inclusions of glassy to crystalline texture. The large boulders (0.2 m and larger) are mainly light-matrix breccias (B_1, B_2 of Wilshire and others, this volume); many have well-rounded profiles and have accumulated deep fillets of soil by erosion of their friable surfaces. Similar rocks occur as possible outcrops in the upper half of the crater wall. Dark-matrix rocks (B_4, B_5) make up 10 to 30 percent of the boulders present and appear to be very resistant. to erosion. Generally perched or sitting within shallow depressions, they are interpreted as the deepest material exposed in the crater wall and therefore the latest to be deposited on the crater rim.

The small fragments (2 to 25 g) collected in soils and rake samples reflect in part, the more resistant components contained interstitially and as clasts within the larger boulders. These include the coherent dark- and intermediate-gray (B_3) breccias, metaclastic (C_2) rocks, and holocrystalline fragments with igneous textures (C_1 of Wilshire and others). The metaclastic and holocrystalline rocks were documented from the matrix of only one boulder, the dark-matrix breccia called Outhouse rock. Light-matrix breccias and glass-coated fragments (G) are common locally in the smaller samples and as clasts from the dark-matrix breccias.

The sample suite is divided into four subgroups based on their locations. Three are on the rim crest of North Ray, the fourth is near the edge of the continuous ejecta blanket. Of 148 rock samples, only a fourth weigh more than 25 g, but these probably represent the abundance and distribution of rock types more accurately than do the smaller fragments. Light-matrix breccias characterize two of the three rim crest areas; dark-matrix breccias with associated metaclastic and igneous inclusions are typical of the large dark boul-

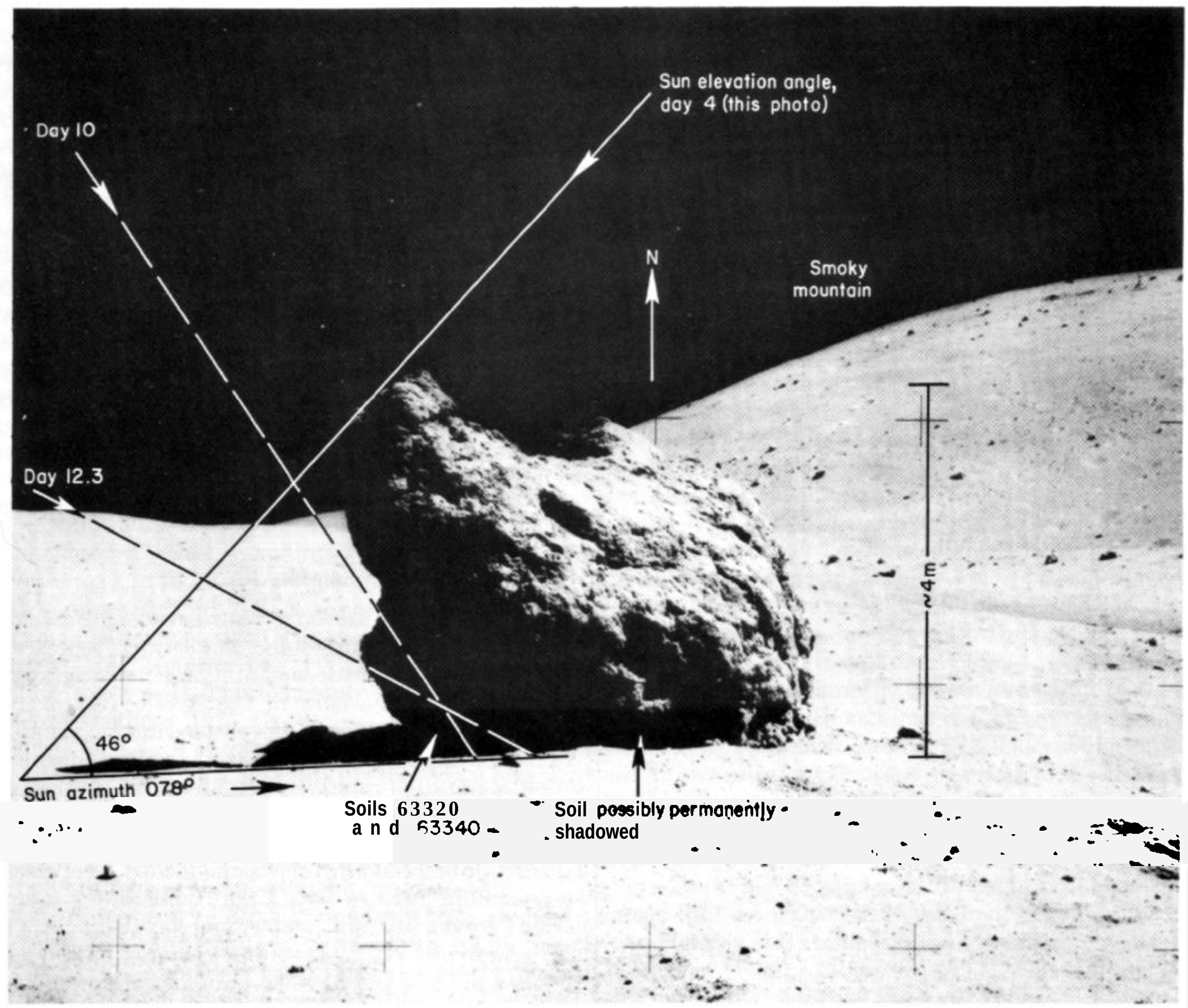

FIGURE 34.-Estimated exposure to sunlight beneath overhang of Shadow rock during one lunation. Predicted sun-elevation angles (dashed lines) for earth days 10 and 12.3 correspond to inclined surface on Shadow rock above soil sample 63320. Angle error due to changing sun azimuth is 2° to 3°. AS16-106-17393.

ders at one rim crest site and at station 13, 0.75 km away. Shadow rock, at station 13, appears atypical of the normally light-colored block population on the outer rim. It is therefore interpreted as part of a discontinuous ray extending southeast from the crater rim. The light-matrix materials that constitute the main fragment population are derived from at least the upper half of North Ray (possibly deeper) and overlie a zone of dark material indicated by a small mound on the crater floor. The stratigraphic implications for other parts of the landing site are discussed by Ulrich and Reed (this volume).

The generally thin regolith (about 1 cm) thickens to 15 cm or more where it forms fillets around the friable light-matrix boulders. The soils on this fresh crater rim are generally very light gray but not as light as those immediately beneath the surface. Their mineral compositions, while distinct from other areas, are reported to be very similar within the North Ray ejecta blanket. Mass movement on the steep crater wall and rim has transported soil and a few blocks toward lower areas.

Magnetic readings from the Lunar Portable Magnetometer were high where measured at station 13. They are believed (Strangway and others, 1973) to reflect moderately welded breccias that were emplaced and cooled from temperatures higher than 700°C in a field of a few thousand gammas. In view of the apparent lack of remanent magnetization in more crystalline rocks, it is suggested here that the magnetic field was very short lived and was induced by a large local or regional impact event affecting only melt-rich breccias that cooled rapidly, thereby retaining the transient field.